Population coding under the scale-invariance of high-dimensional noise

S. Amin Moosavi[1*], **Sai Sumedh R. Hindupur**[2], **Hideaki Shimazaki**[3,4*]

***For correspondence:**
aminmoosavi@g.ucla.edu (S.A.M.);
h.shimazaki@i.kyoto-u.ac.jp (H.S.)

[1]Departments of Neurobiology, David Geffen School of Medicine, University of California, Los Angeles, Los Angeles CA 90095, USA; [2]School of Engineering and Applied Sciences, Harvard University, Cambridge, Massachusetts, USA; [3]Graduate School of Informatics, Kyoto University, Kyoto, Japan; [4]Center for Human Nature, Artificial Intelligence, and Neuroscience (CHAIN), Hokkaido University, Sapporo, Japan

Abstract High-dimensional neural activities exhibiting scale-invariant, power-law noise spectra are ubiquitously observed across various brain regions and species. However, their impact on information coding remains unclear. We provide scaling conditions for noise covariance that clarify the boundedness of information and establish a quantitative relation between information capacity and population size, based on the properties of scale-invariant noise covariance observed in stimulus-evoked activities of mouse V1 neurons. Our analysis reveals that sublinearly scaling small noise components align sufficiently with the signal direction, enabling neurons to convey stimulus information unboundedly as population size increases. These findings demonstrate that the quasi-universal scaling of neural noise covariance lays a foundation for understanding the scaling and boundedness of population codes, highlighting the critical need to consider the full spectrum of high-dimensional noise.

Neural activity is highly variable yet structured in high-dimensional space [1–3], ubiquitously exhibiting quasi-universal, scale-invariant power-law eigenvalue spectra of noise covariances across various brain regions and species [4–6]. Recent advances in theoretical and empirical studies suggest potential mechanistic and functional origins of the scale-invariant properties [4–8]. However, the impact of the high-dimensional noise on population coding remains poorly understood.

Early studies of neuronal activity in the monkey MT area revealed that the activity of single neurons is highly informative about the animal's perceptual sensitivity in discriminating stimulus directions [9,10], suggesting that neurons encode stimuli in an overly redundant manner. In redundant coding, the information conveyed about a stimulus increases sublinearly as the size of the neural population grows, in contrast to the linear increase observed with independent coding [10,11]. A hallmark of the redundant coding is shared noise in neural activity across repeated trials, which obscures the signal, quantified by the change in the average population activity in response to a stimulus change [12–14]. Recent high-throughput techniques for the simultaneous recording of hundreds or thousands of neurons have made it possible to visualize the sublinear increase in the conveyed information as a function of the observed number of neurons [15–18].

Redundant coding can be so strong that it may limit information: Coded information may saturate at its maximum value in the limit of a large number of neurons [10,19,20]. To clarify how high-

dimensional noise impacts the boundedness of information scaling in significantly larger networks beyond observed populations, here we develop a population coding theory based on the scaling properties of noise covariance. We provide the necessary and sufficient condition for the scaling of noise covariance that ensures the boundedness of information and clarifies its relationship to a unique noise structure that has been suggested to limit information [21]. This condition highlights the critical need to consider the full spectrum of high-dimensional noise when predicting the scaling and boundedness of information coding in large neuronal populations. We further establish a connection between the scaling of the covariance eigenvalue spectrum, its power-law exponent, the directional properties of noise components relative to a signal, and their effects on coded information.

We assessed information scaling in large-scale recordings of mouse V1 neurons [22], based on the observed scale-invariant noise spectra and the power-law relationship between the magnitude and orientation of the noise components relative to a signal. The approach transcends earlier large-scale studies [15–18,22] by replacing oversimplified assumptions about covariance scaling with the quasi-universal scaling observed in the data. Consequently, while these studies reported that information is bounded in large neural populations, we show that noise correlations, despite their detrimental effect on stimulus coding, do not limit the information. Therefore, neural populations have the capacity to encode stimulus information without bounds. These results demonstrate that the quasi-universal scaling of neural noise covariance provides a foundation for revealing the scaling and boundedness of population codes.

Results

Small noise components determine the boundedness of information in subsampled populations

The relationship between a signal and noise in the activity of N neurons evoked by multiple presentations of a stimulus (s) is represented in an N-dimensional space, where each dimension corresponds to the activity of a single neuron (Fig. 1a). In this space, a vector $\mathbf{f}_N(s) = (f_1(s), f_2(s), \dots, f_N(s))^{\mathrm{T}}$ represents trial-averaged ensemble activity, and the signal denoted by $\mathbf{f}'_N(s)$ is an infinitesimal change in $\mathbf{f}_N(s)$ caused by a small change in the stimulus. Noise is the deviation from $\mathbf{f}_N(s)$ during each stimulus presentation, quantified by a noise covariance matrix $\mathbf{\Sigma}_N$ that is represented by its eigenvectors $\mathbf{u}_{i,N}$ and eigenvalues $\lambda_{i,N}$ where $i = 1, \dots, N$. These eigenvalues are indexed in descending order: $\lambda_{1,N} \geq \lambda_{2,N} \geq \cdots \geq \lambda_{N,N}$. The overlap between $\mathbf{f}'(s)$ and each $\mathbf{u}_{i,N}$ is measured by the angle $\theta_{i,N}$ between the two vectors (Fig. 1b).

The coding capacity is quantitatively measured by the linear Fisher information (LFI) [13,19–21,23] formulated as:

$$I_N = \sum_{i=1}^{N} \frac{|\mathbf{f}'_N(s)|^2}{\lambda_{i,N}} \cos^2\theta_{i,N}. \tag{1}$$

The LFI gives an upper bound of information that linear decoders can read out. The contribution of each noise component to the LFI is measured by $\cos^2\theta_{i,N}$ termed angular occupation, which satisfies $\sum_{i=1}^{N} \cos^2\theta_{i,N} = 1$. Noise components having direction toward the signal $\mathbf{f}'_N(s)$ ($\cos^2\theta_{i,N} \neq 0$) contribute to LFI with a magnitude depending on the noise strength. In correlated neuronal populations, the alignment of $\mathbf{f}'_N(s)$ with eigenvectors with larger eigenvalues impairs the coding accuracy, and alignment with smaller eigenvalues improves the coding accuracy, compared to independent neurons.

We examine the scaling of the LFI when the subpopulation size N changes. The subpopulation is constructed by randomly subsampling N neurons from a total of N_t recorded neurons ($N \leq N_t$). The signal magnitude $|\mathbf{f}'_N(s)|^2$ scales linearly with N under the random subsampling as long as a finite fraction of its elements is positive because $|\mathbf{f}'_N(s)|^2$ is a summation of N nonnegative variables. Whether the LFI is limited depends on how $\lambda_{i,N}$ scales against the linear $|\mathbf{f}'_N(s)|^2$ and how the angular occupation $\cos^2\theta_{i,N}$ changes with N. From here onward, we categorize the covariance eigenvalues

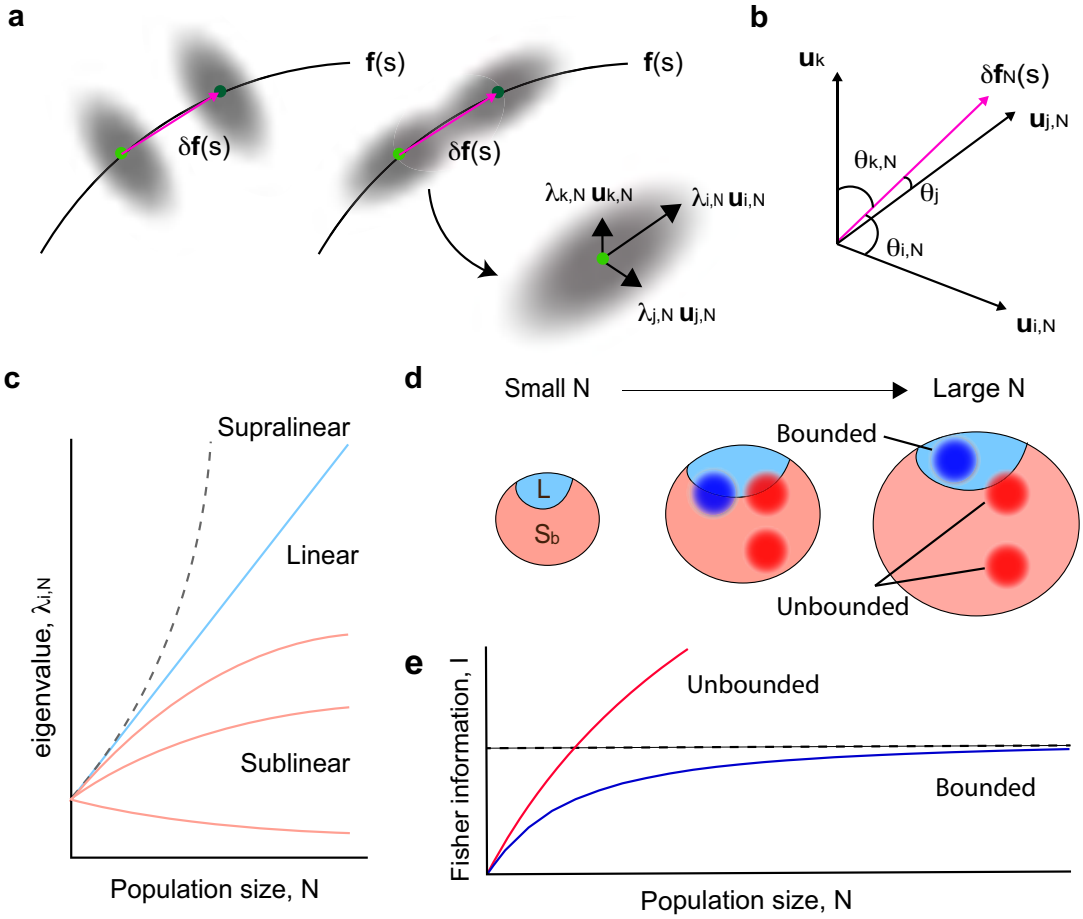

Fig. 1. Schematic illustrating necessary and sufficient conditions for bounded and unbounded LFI. a, A schematic of a subspace spanned by three neurons. The mean activity of neurons $\mathbf{f}_N(s)$ encodes the stimulus s as first-order statistics (solid black line). In addition to the change in the mean responses (green dots) to the two close stimuli ($\delta\mathbf{f}_N(s)$, magenta arrow, a finite size analog of $\mathbf{f}'(s)$), the co-variability (gray areas) affects stimulus coding beneficially (left) or detrimentally (right) when compared to circular independent noises. Noise covariance is quantified by eigenvectors $\mathbf{u}_{i,N}, \mathbf{u}_{j,N}, \mathbf{u}_{k,N}$ and their respective noise strength $\lambda_{i,N}, \lambda_{j,N}, \lambda_{k,N}$. **b**, A three-dimensional view of the orientation of $\delta\mathbf{f}_N(s)$ with respect to the covariance eigenvectors. $\theta_{i,N}$ is the angle between $\delta\mathbf{f}_N(s)$ and the eigenvector $\mathbf{u}_{i,N}$. **c**, Supralinear, linear, and sublinear eigenvalues as a function of N. Supralinear eigenvalues are prohibited for subsampled populations. **d**, Schematic representation of the necessary and sufficient condition. Three large circles indicate a set of eigenvalues for small, medium, and large-size neuronal populations, respectively, with L and S_b representing the sets of linear and sublinear eigenvalues. The area size indicates the set cardinality (dimensionality). Blue and red smaller circles indicate neural populations with bounded (blue) and unbounded (red) information. The overlap between the circles with each set explains the contribution of each set to the information via nonzero angular occupation. For the LFI to be bounded (blue circle), the overlap with the sublinear set must decrease faster than a critical value set by the scaling of sublinear eigenvalues with increasing subpopulation size. Otherwise, the LFI is unbounded (red circles). **e**, Bounded (blue) and unbounded (red) LFI.

based on their scaling behavior versus N as supralinear, linear, and sublinear eigenvalues (Fig. 1c, see Supplementary Note 1 for definition).

The sum of covariance eigenvalues gives the total variance of the N neurons' activity, i.e., the sum of the individual variances of all neurons. Since the variance of single-neuron activity is independent of the size of the subsampled population N, we expect that

$$\sum_{i=1}^{N} \lambda_{i,N} \sim N. \tag{2}$$

This adds a few crucial constraints to the eigenspectrum of the covariance matrix (Supplementary Note 1). First, the subsampled systems lack supralinear eigenvalues. Second, the number of linear eigenvalues must converge to a fixed finite number with increasing N; otherwise, their sum grows supralinearly. Third, the number of sublinear eigenvalues must increase indefinitely with the subpopulation size; thus, they dominate the spectrum in large-N limit. Linear eigenvalues if they exist, appear at early indices in the eigenspectrum in descending order, followed by the sublinear eigenvalues.

Given these constraints, we provide the necessary and sufficient condition for both bounded and unbounded LFI (Methods and Supplementary Note 2). This condition reveals that the alignment of linear eigenvalues with a signal is only a necessary condition for the LFI to be bounded. For the LFI to be either bounded or unbounded, the angular occupations by the eigenvectors associated with the dominant sublinear eigenvalues must respectively decrease faster or slower than a critical rate as N increases (Fig. 1d,e). Here, the magnitudes and angles of the sublinear noise components determine the critical rate, highlighting the necessity of examining the behavior of smaller eigenvalues of the neural activities to reveal their information capacity.

Noise covariance scaling of mouse V1 neurons suggests unbounded information coding

We analyzed stimulus-responses of the mouse V1 neurons[22] obtained in the experiments designed to examine their ability to detect small changes in angles of grating stimuli (Fig. 2a). The dataset includes 37,224 - 50,954 neurons recorded from five mice with ∼1000 repeated trials per degree while animals passively view stimuli. These neurons exhibited linearly scaling $|\mathbf{f}'_N|^2$ (Fig. 2b,c), as expected. Figure 2d shows that the eigenspectrum of the noise covariance matrix scales with the subpopulation size. By introducing a normalized index $x_i = i/N$, the eigenspectrum is in agreement with the following scale invariance (Fig. 2e,f),

$$\lambda_{i,N} = N^{-\alpha} g(x_i), \tag{3}$$

where $\alpha > 0$, and $g(x_i)$ is given by

$$g(x_i) = x_i^{-\alpha} \left(\frac{x_i}{b}\right)^{x_i - 1} \exp\left[a(-x_i \log x_i)^{\nu} + c\right]. \tag{4}$$

The exponential function accounts for the cutoff that occurs at $x_i = 1$ by definition, whereas the power-law part explains the behavior of larger eigenvalues at $x_i \to 0$ limit. While the functional form of $g(x_i)$ is independent of N, its domain $x_i \in [1/N, 2/N, \ldots, 1]$ depends on N. The exponent α, obtained by finite-size scaling collapse of data (see Methods), appears quasi-universal among all the mice in the experiment ($\alpha = 0.178 \pm 0.013\mathrm{SD}$, Extended figures 1-5). In contrast, other fitted parameters vary across mice.

The equations above specify the behavior of eigenvalues in the large N limit. The larger eigenvalues at the low indices ($x_i \ll 1$) exhibit power-law scaling as $g(x_i) \sim x_i^{-(1+\alpha)}$, which results in the linear eigenvalues $\lambda_{i,N} \sim N^{-\alpha} x_i^{-(1+\alpha)} \sim N$ for any fixed $i \ll N$. In other words, if we consider the first N_c eigenvalues where N_c is a fixed value, they increase linearly with N because $x_{N_c} = N_c/N \to 0$. Similarly, for the i-th eigenvalues with an integer $i \leq N^{\beta}$ and $0 \leq \beta < 1$, we have $x_i = N^{\beta}/N \to 0$ in the large N limit. The eigenvalue at an integer $i = N^{\beta}$ scales as $\lambda_{i,N} \sim N^{-\alpha} x_i^{-1-\alpha} \sim N^{1-\beta(1+\alpha)}$, which is

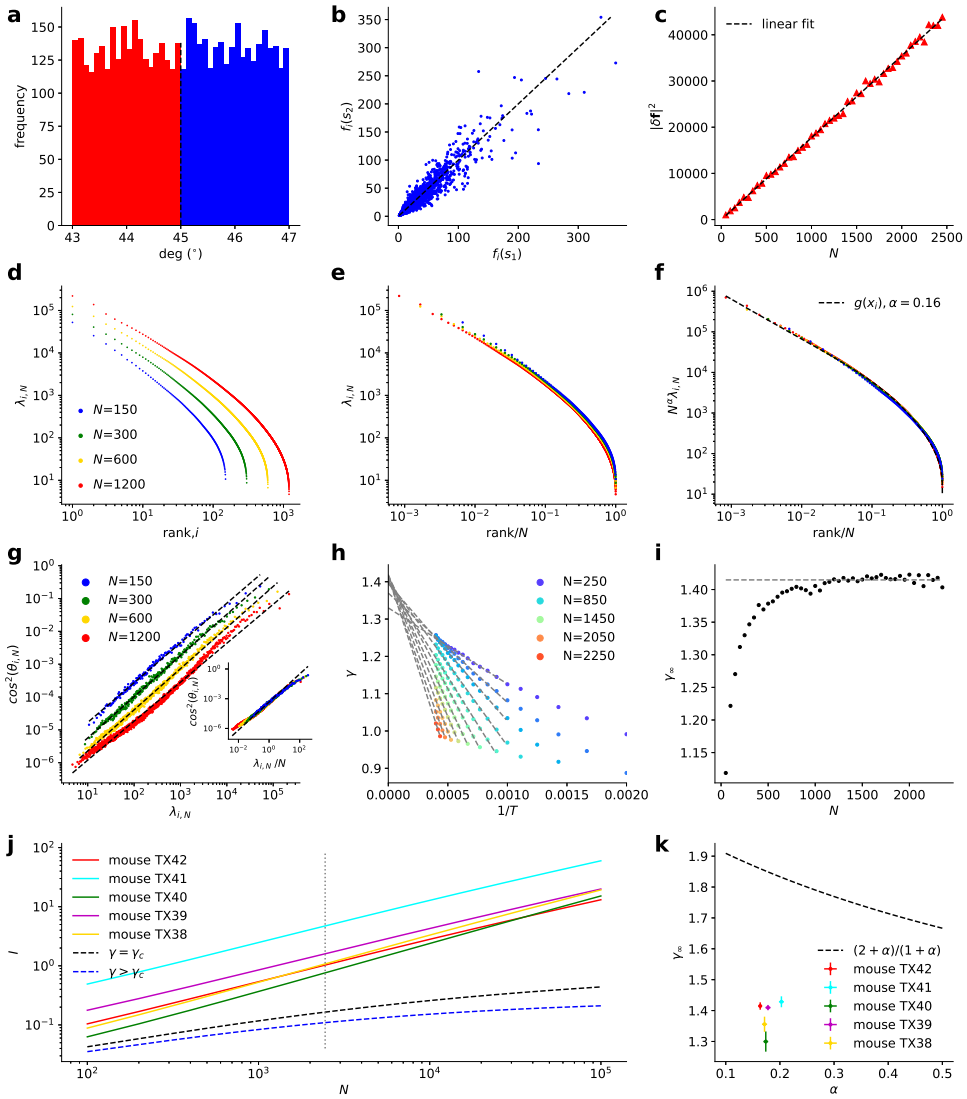

Fig. 2. Scaling analysis of mouse V1 neurons. a, A frequency histogram of grating stimulus orientations presented to mouse TX42. The stimuli with orientations $43° - 45°$ (red) are categorized as Stimulus 1 and those with $45° - 47°$ (blue) as Stimulus 2. **b**, Comparison of mean responses of neurons $f_i(s)$ (i=1,...,18982) to the Stimulus 1 ($s = s_1$) and 2 ($s = s_2$) for mouse TX42. $f_i(s)$ is the average of each category's stimuli (trials). The dashed line is a diagonal. **c**, Mean response changes, $|\delta f_i|^2$ vs the subpopulation size N, where $\delta f_i = f_i(s_1) - f_i(s_2)$, for mouse TX42. $|\delta f_i|^2$ is an average over 200 randomly selected subpopulations of size N. The dashed line indicates a linear fit. **d**, Noise eigenspectra for different subpopulation sizes N in mouse TX42. **e**, Eigenspectra vs the normalized rank, $(x_i =)i/N$. **f**, Rescaled eigenspectra by multiplying N^α. The dashed line represents the fitted $g(x_i)$, (Eq. 3). The fitted scaling parameter is $\alpha = 0.164 \pm 0.002$. The fitted parameters of $g(x_i)$ are $a = 2.752$, $b = 9.611$, $c = 2.298$, and $\nu = 0.254$. **g**, $\cos^2\theta_{i,N}$ vs $\lambda_{i,N}$ for different N in mouse TX42 using all trials (2500 per stimulus). The dashed lines indicate a linear fit. (Inset) $\cos^2\theta_{i,N}$ vs the scaled eigenvalue, $\lambda_{i,N}/N$. **h**, Fitted exponent γ in Eq. 5 as a function of $1/T$ for different N, where T is the number of trials. The solid lines indicate fitted linear functions. The intercepts estimate γ at an infinitely large number of trials. **i** The intercept γ_∞ for different N. The average γ_∞ for $N = 1000 - 2500$ (dashed line) was 1.415 ± 0.006. **j**, Inferred LFI for mouse TX42 and the other four mice (solid lines) as a function of N in the log-log plot. The LFI was computed from Eqs. 3 and 5, using the parameters fitted to each mouse. The dashed lines are theoretical LFI resulting in critical (black, $\gamma = \gamma_c$) and bounded information (blue, $\gamma < \gamma_c$) for mouse TX42. The vertical dashed line is the number of neurons used to estimate the parameters. **k**, Estimated γ_∞ vs α for all mice. The dashed line indicates the critical boundary (Eq. 6), below which the LFI is unbounded. The error bars are 2SD.

a sublinear function of N for $\beta > 0$. These results indicate that the eigenspectrum contains a finite set of linear eigenvalues, followed by dominant sublinear eigenvalues.

The alignment of the noise eigenvectors linked to linear or sublinear eigenvalues with $\mathbf{f}'(s)$ determines whether the LFI is bounded. The angular occupations $\cos^2\theta_{i,N}$ and eigenvalues $\lambda_{i,N}$ show linear dependency on a logarithmic scale (Fig 2g), indicating another scale-invariant relation:

$$\cos^2\theta_{i,N} = \frac{\lambda_{i,N}^{\gamma}}{\sum_{i'=1}^{N}\lambda_{i',N}^{\gamma}}. \tag{5}$$

The eigenvectors tied to the larger eigenvalues occupy a large portion of the angular occupations, indicating that the linear eigenvalues align with $\mathbf{f}'(s)$ and potentially limit the information. On the contrary, the eigenvectors associated with the smaller eigenvalues exhibit smaller angular occupations (nearly orthogonal to $\mathbf{f}'(s)$). Yet, due to the sub-linearity, their contributions to the coded information can be significant. From Eqs. 1 and 2, one can see $I_N \sim N$ if $\gamma = 1$ and $I_N \to const.$ for $\gamma = 2$ (Supplementary Note 3). Therefore, a critical exponent $\gamma = \gamma_c$ exists between one and two, where the information changes behavior from unbounded to bounded. We find that this critical exponent is given by

$$\gamma_c = \frac{2+\alpha}{1+\alpha}. \tag{6}$$

Specifically, in the large N limit the LFI scales as

$$I_N \sim \begin{cases} \text{const.} & \gamma > \gamma_c \\ \log N & \gamma = \gamma_c \\ N^{2-\alpha(\gamma-1)-\gamma} & 1 \le \gamma < \gamma_c. \end{cases} \tag{7}$$

For $\alpha = 0.164$ of the mouse TX42, the critical exponent is $\gamma_c = 1.859$. The exponent γ estimated by extrapolating the sample size is $\gamma = 1.415 \pm 0.006$ (Fig. 2h,l). As it is smaller than γ_c, the result indicates that the LFI of the neurons in this dataset increases unboundedly. Moreover, the LFI asymptotically scales as a power-law with the exponent $2-\alpha(\gamma-1)-\gamma = 0.517$, which is a sublinear but unbounded function of N. Such sublinear, unbounded behavior was consistently observed across all five mice (Fig. 2j,k; See Extended Figures 1-5 for individual results). Accordingly, we conclude that the mouse V1 neurons' correlated activity causes redundancy, yet it is insufficient to limit information in the large N limit. Therefore, the only constraints on the information capacity are the limited stimulus information available in the retina[24] and the total number of neurons in the V1 and related areas, which are not imposed in this theory.

Under the scale invariance with $\alpha > 0$ (Eq. 3), the selected functional form for $g(x_i)$ in Eq. 4, specifically $g(x_i) \sim x_i^{-(1+\alpha)}$ in the $x_i \to 0$ limit, not only allows linear eigenvalues but also aligns with the linear scaling of the total variance (Eq. 2). Generally, given the power-law scaling $g(x_i) \sim x_i^{-\mu}$, we proved that the constraint of the linear total variance (Eq. 2) leads to $\mu = 1+\alpha$ if α is positive (Supplementary Note 4 and 5, and Table 1). In this case, the leading eigenvalues scale linearly, $\lambda_{i,N} \sim N$ ($i \ll N$). On the contrary, this constraint imposes $\mu < 1$ if $\alpha = 0$, indicating that the slope must be shallower than 1 if the eigenspectra in the normalized index collapse in the limit of large N. In this case, the leading eigenvalues scale sublinearly, $\lambda_{i,N} \sim N^{\mu}$ ($i \ll N$). This means that all

Scaling parameter α	Power-law exponent μ	Scaling of leading eigenvalues	Linear Fisher information
$\lambda_{i,N} = N^{-\alpha} g(x_i) \quad (x_i = i/N)$	$g(x_i) \sim x_i^{-\mu} \quad (x_i \ll 1)$	$\lambda_{i,N} \sim N^{\mu-\alpha} \quad (i \ll N)$	I_N
$\alpha > 0$	$\mu = 1+\alpha > 1$	$\lambda_{i,N} \sim N$ (linear)	bounded/unbounded
$\alpha = 0$	$\mu < 1$	$\lambda_{i,N} \sim N^{\mu}$ (sublinear)	unbounded

Table 1. The relationship among the scaling parameter α, the power-law exponent μ, and the scaling of leading eigenvalues of a scale-invariant power-law eigenspectrum, and their connection to the boundedness of the linear Fisher information under the linear scaling of the total variance.

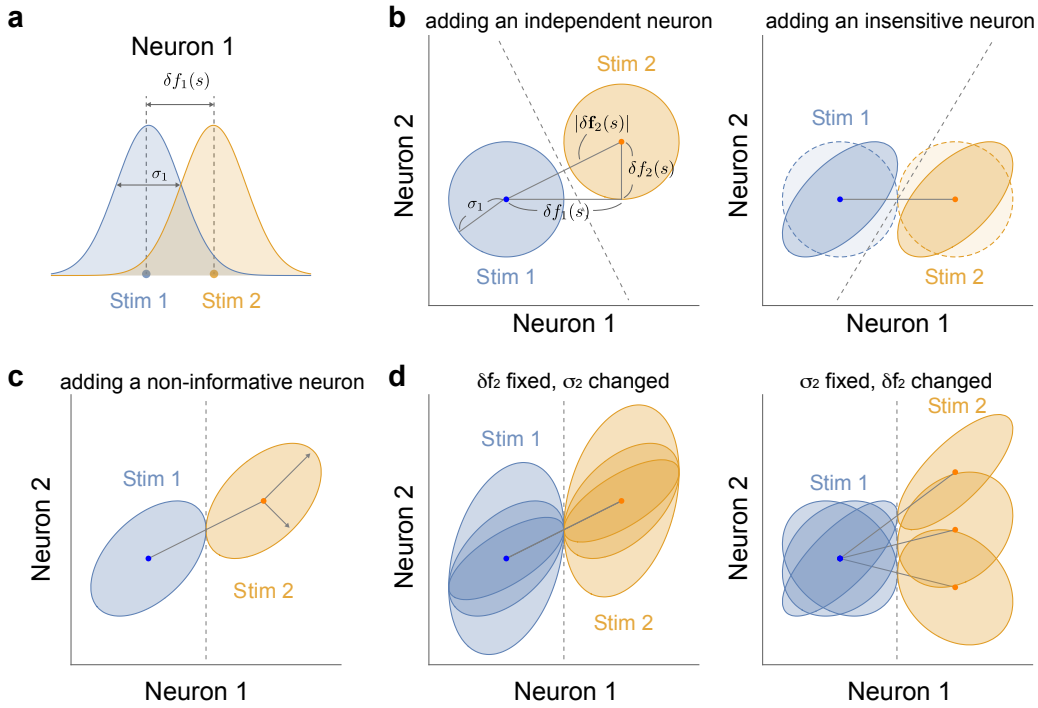

Fig. 3. Incremental effect of adding a neuron on stimulus coding. a, Response distributions of a single neuron (Neuron 1) for two close stimuli (blue for Stimulus 1 and orange for Stimulus 2). The standardized mean difference $\delta f_1(s)/\sigma_1$ quantifies the ability to discriminate between the two stimuli. **b**, (Left) Joint distributions of two neurons after adding an independent, stimulus-sensitive neuron (Neuron 2) to Neuron 1 with the same variance ($\sigma_2 = \sigma_1$). The dashed line indicates the optimal linear decision boundary. The circle radius indicates one standard deviation. The distance between the mean responses for the two stimuli is $|\delta \mathbf{f}_2(s)| = \sqrt{\delta f_1(s)^2 + \delta f_2(s)^2}$. (Right) Joint distributions of two neurons (solid blue and orange for Stimuli 1 and 2, respectively) after adding a correlated, stimulus-insensitive neuron (Neuron 2), having the same variance ($\sigma_2 = \sigma_1$). Neuron 2 does not change the mean activity, while the correlation results in ellipsoidal distributions. The dashed line is an optimal decision boundary for the correlated neurons. Light blue and orange circles result from adding an independent, stimulus-insensitive neuron for comparison. **c**, Joint distributions of two neurons after adding a noninformative neuron (Neuron 2). Adding a correlated, stimulus-sensitive neuron does not increase discriminability from the single neuron's performance when $(\delta f_1(s)/\sigma_1^2)(\rho\sigma_1\sigma_2) = \delta f_2(s)$. We impose $\delta f_1^2/\sigma_1^2 > \delta f_2^2/\sigma_2^2$ to make the LFI of Neuron 2 smaller than that of Neuron 1. **d**, Variations of the joint distributions not changing the stimulus discriminability. (Left) The change in the mean response of Neuron 2 ($\delta f_2(s)$) is fixed, whereas its variance σ_2 and correlation varied while preserving the LFI. (Right) The variance of Neuron 2 is fixed, whereas Neuron 2's mean response change ($\delta f_2(s)$) and correlation varies while preserving the LFI.

eigenvalues scale sublinearly, making the information an unbounded function of N, regardless of the behavior of angular occupations. Indeed, when neural activities are individually normalized by their non-zero mean activities[6] or standard deviations[4,5], we observed that the slopes of leading eigenvalues satisfy $\mu < 1$ (Extended Figure 6), further supporting that the LFI is not bounded in this data set.

Differential correlations limit the LFI of subsampled populations

While we provided the scaling conditions for bounded and unbounded information under the linear scaling of the total variance, it has been suggested that the presence or absence of a specific noise structure known as differential correlations determines the boundedness of information[21]. We prove that these two conditions are not in general equivalent, but become identical under the subsampling constraint. For this goal, we first quantitatively explain how the addition of a subsampled neuron to a population changes or does not change the LFI.

Recursively adding a neuron to a population creates a subsampled population whose covariance matrix includes the covariance matrix of a smaller subsampled population, forming a nested structure. Given N neurons, consider adding a single neuron whose mean response, variance, and covariance with the existing N neurons is given by $f_{N+1}(s)$, Σ_{N+1}, $\mathbf{c}_N$, respectively. The LFI of $N+1$

neurons is given by (Supplementary Note 6)

$$I_{N+1} = I_N + \omega_{N+1}^{-1} \left(\mathbf{f}'_N(s)^{\mathrm{T}} \mathbf{\Sigma}_N^{-1} \mathbf{c}_N - f'_{N+1}(s) \right)^2 , \tag{8}$$

where $\omega_{N+1} = \Sigma_{N+1} - \mathbf{c}_N^{\mathrm{T}} \mathbf{\Sigma}_N^{-1} \mathbf{c}_N$. Since $\omega_{N+1} > 0$ for the covariance of $N+1$ neurons to be positive definite, Eq. 8 indicates that the LFI of the subsampled population is a nonincreasing function of N. Further, Eq. 8 reveals two distinct ways to increase the LFI (Fig. 3a,b). First, when adding an independent neuron (i.e., $\mathbf{c}_N = \mathbf{0}$), the LFI increases by $\Sigma_{N+1}^{-1} f'_{N+1}(s)^2$, that is the LFI of the added neuron (Fig. 3b left). Second, the LFI increases even if $f'_{N+1}(s) = 0$, namely even if we add a neuron whose activity is insensitive to the stimulus change, it will contribute to increasing information as long as $\mathbf{f}'_N(s)^{\mathrm{T}} \mathbf{\Sigma}_N^{-1} \mathbf{c}_N \neq f'_{N+1}(s)$. This is because adding a correlated neuron can remove the overlap of the noise distributions for the two close stimuli (Fig. 3b right), explaining an effect found in the sensory and frontal areas of rodents and primates [25–29].

Moreover, the LFI does not increase if $\mathbf{f}'^{\mathrm{T}}_N \mathbf{\Sigma}_N^{-1} \mathbf{c}_N = f'_{N+1}(s)$ (Fig. 3c,d). To keep the LFI fixed, the noise variance along $\mathbf{f}'_N(s)$ must scale with N as the squared distance between two stimuli (i.e., $|\mathbf{f}'_N(s)|^2$) scales with N. We further note that the LFI is an infinitesimal value of the squared standard mean difference along the optimal decision line, a line perpendicular to an optimal decision boundary (Supplementary Note 6). This decision boundary is independent of the activity of an added neuron when the LFI remains unchanged.

Moreno-Bote et al. [21] showed that LFI is limited if the noise covariance of neurons is represented as

$$\mathbf{\Sigma}_N = \mathbf{\Sigma}_N^0 + \epsilon \mathbf{f}'_N(s) \mathbf{f}'^{\mathrm{T}}_N(s), \tag{9}$$

where ϵ is a constant and $\mathbf{\Sigma}_N^0$ is any covariance matrix whose respective information $I_0 = \mathbf{f}'_N(s)^{\mathrm{T}} (\mathbf{\Sigma}_N^0)^{-1} \mathbf{f}'_N(s)$ diverges with N. The rest is defined as the differential correlations that limit the LFI below ϵ^{-1} with the form:

$$I_N = \frac{I_0}{1 + \epsilon I_0}. \tag{10}$$

They further proposed that only differential correlations can limit the information. However, the original proof was restricted to specific noise covariances, leaving the claim unsubstantiated for general covariance matrices. Here, based on Eq. 8, we prove that, in general, the noise covariance of subsampled populations exhibiting increasing and saturating LFI can always be expressed in the form of Eq. 9 (Supplementary Note 7). In other words, such noise covariance inherently contains differential correlations. This result supports the widespread use of the concept led by differential correlations [24,30,31]. Importantly, however, the proof of equivalence between the necessary and sufficient condition (Methods and Supplementary Note 2) and the presence of differential correlations for subsampled populations also mitigates the need to directly search for differential correlations to confirm or refute the boundedness of information. Moreover, differential correlations are absent in the more general noise covariance of non-subsampled neuronal populations even when they exhibit the linear scaling of the total variance and express finite limiting LFI, e.g., when the LFI is a nonincreasing function of N (Supplementary Note 8). Such a scenario might occur in growing neuronal populations, for example, through neurogenesis.

Given their identity under the subsampled conditions, we can reconfirm the necessity of the linear eigenvalues for the bounded LFI as a consequence of the differential correlations [21,30]. Namely, the addition of differential correlations induces one or multiple linear eigenvalues in the covariance matrix, depending on whether $\mathbf{\Sigma}_N^0$ is unbounded for all signal directions or not (Supplementary Note 9). However, to further achieve sufficiency, this alignment must occur faster than the rate set by the sublinear noise components (Methods, Supplementary Note 2).

Discussion

We proposed a theory of population coding based on the scaling properties of neural systems, which allowed us to predict the boundedness of information. This theory critically considers the

constraints introduced by random subsampling, leading to the following key findings: (i) The square distance between mean responses of randomly subsampled N neurons to two close stimuli increases proportionally to N [16,18]. (ii) The linear increase in total variance allows only a finite number of noise components to scale linearly, while the rest scales sublinearly. (iii) LFI is limited if the sublinear eigenvalues' angular occupation drops faster than a rate set by these sublinear noise components. Applying these constraints, we showed that (iv) a scale-invariant noise eigenspectrum with $\alpha > 0$ or $\alpha = 0$ necessitates that the power-law spectrum decays with an exponent μ greater or less than one, respectively. (v) Only the scale invariance with $\alpha > 0$ allows for linear eigenvalues, which can potentially limit the information. (vi) Conversely, $\alpha = 0$ only allows for sublinear eigenvalues, resulting in unbounded LFI. Through examination of mouse data, we found the scale-invariant noise eigenspectra with $\alpha > 0$ (Fig. 2d-f) and another novel scaling power-law relation between the eigenvalues and angular occupations with an exponent γ (Fig. 2g). Our analysis identified the critical exponent above and below which the LFI becomes bounded or remains unbounded. We found that the directions of the sublinear noise components in the mouse data overlap with the signal direction at a sufficient rate, leading to a sublinear yet unbounded increase in LFI. Consequently, we conclude that the information encoded in the mouse V1 neurons can continue to increase unboundedly, overarching the previous study on this dataset that reported no apparent signs of saturation in the LFI lower bound up to the recorded number of neurons [22].

Previous studies [15,16,18,22] reporting bounded information in the limit of large networks are based on inadequate assumptions on covariance scaling. First, the study reported the high-precision coding [22] that provided the data we analyzed in this study relied on extrapolation by a simple parametric scaling with $c_1 + c_2/\sqrt{N}$ fitted to the decoding performance. Our results suggest that the reported bounded precisions in the limit of large N were conservative estimates, as predicted by the authors. Second, ignoring or regularizing the activities related to smaller variances can lead to different and potentially inaccurate conclusions. Rumyantsev et al. proposed saturated information using a dimension reduction method [16]. However, applying the same method to simulated data whose LFI is theoretically unbounded, we observe saturating LFI (Supplementary Note 10, Extended Data Figs. 7 and 8). Third, one can not use Eq. 10 derived from the differential correlations to report the bounded LFI. It is possible to find a saturating function that well fits finite size data because the LFI following Eq. 10 is an arbitrarily increasing and saturating function of N with an unknown saturation value (Supplementary Note 7). Therefore, excellent fits of Eq. 10 to empirical LFI [15,16,18] do not support the boundedness of information.

Our study found scale invariance with a positive α and a fast-decaying power-law exponent $\mu(= 1+\alpha) > 1$ in the recorded neural activities (Fig. 2d-f, and Extended Data Figs. 1-5d-f). In addition, we observed scaling exponent $\mu < 1$ from the covariances of normalized neural activities (Extended Data Figs. 6, 7), further supporting evidence of unbounded information coding. This result aligns with other studies that have reported scale-invariant eigenspectra with scaling exponents less than 1 [4–6,32]. While these results might indicate that noise in neural activities does not generally confound information coding, further rigorous assessment of the scaling parameters α and μ across brain regions and species is necessary to reveal the foundational coding capacities of neurons.

The ongoing activity in the mouse forebrain, including the visual cortex, is high-dimensional [1]. Further, their reliable dimension increases without apparent saturation up to about a million neurons [3]. These findings are consistent with the high-dimensional noise covariances because the ongoing activities driven by the animal's behavior and internal dynamics are likely to cause variability in repeated stimulus-evoked activities [33–35]. The above large-scale analyses showed that the ongoing activities overlap with signal correlations through one or a few-dimensional subspaces, suggesting multiplexed coding by the nearly orthogonal stimulus and spontaneous activities. The present study also supports that the noise correlations, including those arising from measurement noise, do not limit local signal representation. However, in agreement with positive correlations between the signal and noise in early sensory areas reported in other studies [34–38], we found broader directional overlaps between the leading noise components and signal (Fig. 2g), which is neverthe-

less insufficient to limit the information.

More generally, it remains unclear how noises under other specific brain states and behavioral conditions than the passive visual stimulation conditions affect large-scale population coding. In smaller populations, it is known that cortical states[39], locomotion[17,40], and attention[41] modulate noise correlations in a way to improve coding capacity. We showed that population coding is affected by the scaling of smaller noise variances in the population activity and their directions toward the signal. Thus, we can not rule out the idea that even small changes caused by the behavior and internal dynamics[5] in small noise components of the high-dimensional noise have a substantial impact on the stimulus coding fidelity in large-scale neuronal populations.

Methods

Conditions for bounded and unbounded LFI

The subsampled population's LFI (Eq. 1) can be decomposed into the contributions by components with linear and sublinear eigenvalues:

$$I_N = \sum_{i\in L} \frac{|\mathbf{f}'_N(s)|^2 \cos^2\theta_{i,N}}{\lambda_{i,N}} + \sum_{i\in S_b} \frac{|\mathbf{f}'_N(s)|^2 \cos^2\theta_{i,N}}{\lambda_{i,N}}, \tag{11}$$

where L and S_b are sets of linear and sublinear eigenvalues, and $|\mathbf{f}'_N(s)|^2 \sim N$. At large N, the number of elements in set L approaches a constant integer $c > 0$; consequently, the number of elements in set S_b linearly increases with N: $|L| \to c$ and $|S_b| \to \infty$ as $N \to \infty$. The first term converges to a finite value because each individual term in the sum is finite, and the number of linear eigenvalues is also finite. Therefore, the convergence of the second term is the necessary and sufficient condition for the information to be limited. By defining the occupation of $\cos^2\theta_{i,N}$ from sublinear eigenvectors by $W_{S_b}(N) = \sum_{j\in S_b} \cos^2\theta_{j,N}$, the bounded condition can be written as

$$W_{S_b}(N) \left\langle \frac{N}{\lambda_{i,N}} \right\rangle \to const., \tag{12}$$

where the bracket is a weighted average using $\cos^2\theta_{i,N}$ of the sublinear eigenvectors. Namely, the necessary and sufficient condition is that $W_{S_b}(N)$ decreases to zero equal to or faster than $\langle N/\lambda_{i,N}\rangle^{-1}$. This condition can be translated to the condition on the angular occupation by linear eigenvectors $W_L(N)$, using $W_L(N) + W_{S_b}(N) = 1$, such that it must increase faster than the rate.

Consequently, the necessary condition is that $W_{S_b}(N)$ decreases to zero in the large N limit, or equivalently, $W_L(N)$ approaches to one:

$$\lim_{N\to\infty} W_{S_b}(N) = 0, \quad \lim_{N\to\infty} W_L(N) = 1. \tag{13}$$

One can construct populations with unbounded information using the necessary conditions for bounded information. If the eigenspectrum in the normalized index exhibits the power-law spectrum with an exponent $\mu < 1$, the eigenvalues become all sublinear functions: $W_{S_b} = 1$, which violates the necessary condition, resulting in unbounded LFI. For the power-law scaling with $\mu > 1$, the uniform angular occupation ($\cos^2\theta_{i,N} = 1/N$) violates the necessary condition.

Populations with bounded information can be constructed by finding sufficient conditions. An exemplary sufficient condition for the bounded information is obtained as follows. Since $\lambda_{i,N} \geq \lambda_{N,N}$, we obtain the upper bound of $\langle N/\lambda_{i,N}\rangle$ replacing $\lambda_{i,N}$ ($i = 1, \ldots, N-1$) with $\lambda_{N,N}$: $\langle N/\lambda_{i,N}\rangle \leq N/\lambda_{N,N}$. For the information to be bounded, it is sufficient if the upper bound approaches a constant value as N goes to infinity:

$$\lim_{N\to\infty} \frac{W_{S_b}(N)}{\lambda_{N,N}/N} = const, \tag{14}$$

where $\lim_{N\to\infty} \lambda_{N,N}/N = 0$. Consequently, the sufficient condition for the bounded information is that $W_{S_b}(N)$ approaches to zero equal to or faster than $\lambda_{N,N}/N$. Under the scale invariance given by Eqs. 3 and 4, the bound becomes $\lambda_{N,N}/N = N^{-(1+\alpha)}$. For example, if the angular occupation of

the last N^β eigenvalues scales as $\cos^2\theta_{i,N} \approx N^{-\delta}$ ($i = N - N^\beta, \dots, N$), the sufficient condition is met if they decrease as fast as $\delta > 1 + \alpha$. Supplementary Note 2 provides extended descriptions and examples.

Analysis of mouse V1 data

We analyzed two-photon calcium imaging data of mouse V1 neurons from the "full-field" dataset by Stringer et al.[22] (see Data availability). The dataset includes 37,224 to 50,954 V1 neurons from five awake head-fixed mice, passively receiving static grating stimuli with up to ~1000 trials per degree. Each trial presented the static grating stimuli for 750 ms, followed by a gray screen for ~650 ms. The drifting grating stimuli shared the same temporal and spatial frequency (2 Hz and 0.05 cycles per degree, respectively) with an orientation ranging of 43° - 47°. The individual neural activities extracted by the Suite2p toolbox consisted of deconvoluted fluorescence traces responding to the 750 ms stimulus presentation.

We divided the trials into two groups based on the orientation of the grating stimuli. Trials with 43°- 45° (Stimulus 1) comprise the first group, while trials with 45° - 47° (Stimulus 2) comprise the second. The number of trials for Stimulus 1 and 2, L_1, and L_2, differed by a small margin in all datasets (< 50 trials in each data set). We balanced the number of trials for both stimuli by randomly choosing $\min\{L_1, L_2\}$ trials (without replacement) from the stimulus with the larger number of trials. Following this procedure, the number of trials was $1855 - 2654$. Each dataset had $N = 17631 - 21469$ neurons.

We computed the activation means and covariance as follows. Let $x_i^{(r,j)}$ be the activity of the ith neuron at $r(= 1, \dots, R)$th trial under the stimulus presentation $j = 0, 1$. For each group, we estimated the mean activation (trial-average) of all neurons $\hat{\boldsymbol{\mu}}_j = \frac{1}{R}\sum_r \mathbf{x}^{(r,j)}$ ($j = 1, 2$) and their covariance $\mathbf{S}_j = \frac{1}{R}\sum_r (\mathbf{x}^{(r,j)} - \hat{\boldsymbol{\mu}}_j)(\mathbf{x}^{(r,j)} - \hat{\boldsymbol{\mu}}_j)^\mathsf{T}$. We estimated the neurons' covariance as $\mathbf{S} = (\mathbf{S}_1 + \mathbf{S}_2)/2$. To represent the eigenvalues and angular occupations for the subsample size N, we randomly selected subpopulations of size N 200 times and computed the average eigenvalues and angular occupations.

Since the raw activity traces of neurons might include the confoundeing factors such as different expression levels of fluolorecence proteins or positions of neurons in the scanning system, we also constructed the activation means and covariance using the standardized data, by normaling individual neural activity per stimulus by its standard deviation[4,5] or by the mean of the non-zero activities[6] over the trial, r.

Fitting scaling parameters and a scale-invariant function to a eigenspectrum

The scaling parameter of the scale-invariant eigenvalues (Eq. 3) was fitted as follows. The data is composed of the eigenvalues for a range of $N \in \{N_{\min}, N_{\min}+1, \dots, N_{\max}\}$. Given the scale invariance, we must have:

$$\lambda_{i,N_0} = k^\alpha \lambda_{ki,kN_0} \Rightarrow \log \lambda_{i,N_0} = \alpha \log k + \log \lambda_{ki,kN_0}, \tag{15}$$

where $k > 1$ is a positive integer that satisfies $kN_0 < N_{\max}$. Therefore, we define the following cost function for α as

$$C = \sum_{N_0=N_{min}}^{\lfloor N_{max}/2 \rfloor} \sum_{k=2}^{K} \sum_{i=1}^{N_0} \left(\alpha \log k + \log \lambda_{ki,kN_0} - \log \lambda_{i,N_0}\right)^2. \tag{16}$$

The minimum of the cost function is obtained as a solution of $\frac{\mathrm{d}C}{\mathrm{d}\alpha} = 0$ from which we obtain an estimated $\hat{\alpha}$:

$$\hat{\alpha} = \frac{\sum_{N_0=N_{min}}^{\lfloor N_{max}/2 \rfloor} \sum_{k=2}^{K} \sum_{i=1}^{N_0} \log k \left(\log \lambda_{i,N_0} - \log \lambda_{ki,kN_0}\right)}{\sum_{N_0=N_{min}}^{\lfloor N_{max}/2 \rfloor} \sum_{k=2}^{K} N_0 \log^2 k}. \tag{17}$$

We computed $\hat{\alpha}$ for each recording using Eq. 17. We used $N_{min} = 50$ and half of the maximum trial number as N_{max}.

We used the jackknife resampling method to obtain the estimation error of α. For each $r = 1, 2, ..., R$, jackknife replicates $\hat{\alpha}_r$ were generated by computing the mean eigenvalues $\{\lambda^r_{i,N}\}$ over all but the rth repetition, and using them in Eq. 17. Then, the jackknife estimate of the standard deviation of $\hat{\alpha}$ was obtained as $\sqrt{\frac{R-1}{R}\sum_{r=1}^{R}(\hat{\alpha}_r - \hat{\alpha}_{\text{jack}})^2}$, where $\hat{\alpha}_{\text{jack}} = \frac{1}{R}\sum_{r=1}^{R}\hat{\alpha}_r$.

Using the estimated α, we obtained a collapsed curve by plotting $N^\alpha \lambda_{i,N}$ against $x_i = i/N$, using the mean eigenvalues over R repetitions. We then fitted the parametric scale-invariant function $g(x_i)$ (Eq. 4) to the collapsed curve obtained from multiple N values.

The scaling parameter γ (Eq. 5) was estimated as follows. Using t randomly chosen trials for both stimuli (where t was varied from 500 up to the largest number of trials in the recording), we obtained $\gamma(t, N)$ as the slope of a straight line fit to $\cos^2(\theta_{i,N})$ vs $\lambda_{i,N}$ in the log-log plot. For each N, we estimated $\gamma_\infty(N)$ as the y-intercept of a straight line fit to the plot of $\gamma(t, N)$ vs $1/t$. The final estimate $\hat{\gamma}$ and its standard deviation were obtained as the average and standard deviation of $\gamma_\infty(N)$ for $N > 1000$.

Acknowledgments

The authors thank Rubén Moreno Bote, Kenneth Harris, and Quan Wen for valuable discussion, and Magalie Tatischeff and Bingyue Zhu for preliminary data analysis. This work was supported by JSPS KAKENHI Grant Number JP 20K11709, 21H05246.

Authors contributions

S.A.M. and H.S. designed the research; S.A.M., S.S.R.H., and H.S. performed the theoretical analysis. S.S.R.H. and S.A.M. performed the data analysis; H.S. supervised the work. All authors contributed to writing the manuscript.

Declaration of interests

The authors declare no competing interests.

Corresponding authors

Correspondence to S. Amin Moosavi or Hideaki Shimazaki

Data availability

Pachitariu, M., Michaelos, M., and Stringer, C. (2019). Recordings of 20,000 neurons from V1 in response to oriented stimuli. `https://janelia.figshare.com/articles/dataset/Recordings_of_20_000_neurons_from_V1_in_response_to_oriented_stimuli/8279387`

Code availability

The code for the data analysis can be found at `https://github.com/Sai-Sumedh/scaling-population-coding`.

References

[1] Stringer, C. *et al.* Spontaneous behaviors drive multidimensional, brainwide activity. *Science* **364**, eaav7893 (2019).

[2] Lanore, F., Cayco-Gajic, N. A., Gurnani, H., Coyle, D. & Silver, R. A. Cerebellar granule cell axons support high-dimensional representations. *Nat. Neurosci.* **24**, 1142–1150 (2021).

[3] Manley, J. *et al.* Simultaneous, cortex-wide dynamics of up to 1 million neurons reveal unbounded scaling of dimensionality with neuron number. *Neuron* **112**, 1694–1709 (2024).

[4] Meshulam, L., Gauthier, J. L., Brody, C. D., Tank, D. W. & Bialek, W. Coarse graining, fixed points, and scaling in a large population of neurons. *Phys. Rev. Lett.* **123**, 178103 (2019).

[5] Morales, G. B., Di Santo, S. & Muñoz, M. A. Quasiuniversal scaling in mouse-brain neuronal activity stems from edge-of-instability critical dynamics. *Proc. Natl. Acad. Sci. U.S.A.* **120**, e2208998120 (2023).

[6] Wang, Z. *et al.* The geometry and dimensionality of brain-wide activity. *bioRxiv* 2023.02.23.529673 (2024).

[7] Nicoletti, G., Suweis, S. & Maritan, A. Scaling and criticality in a phenomenological renormalization group. *Phys. Rev. Res* **2**, 023144 (2020).

[8] Hu, Y. & Sompolinsky, H. The spectrum of covariance matrices of randomly connected recurrent neuronal networks with linear dynamics. *PLoS Comput. Biol.* **18**, e1010327 (2022).

[9] Britten, K. H., Shadlen, M. N., Newsome, W. T. & Movshon, J. A. The analysis of visual motion: a comparison of neuronal and psychophysical performance. *J Neurosci.* **12**, 4745–4765 (1992).

[10] Zohary, E., Shadlen, M. N. & Newsome, W. T. Correlated neuronal discharge rate and its implications for psychophysical performance. *Nature* **370**, 140–143 (1994).

[11] Averbeck, B. B., Latham, P. E. & Pouget, A. Neural correlations, population coding and computation. *Nat. Rev. Neurosci.* **7**, 358–366 (2006).

[12] Shadlen, M. N. & Newsome, W. T. The variable discharge of cortical neurons: implications for connectivity, computation, and information coding. *J Neurosci.* **18**, 3870–3896 (1998).

[13] Kohn, A., Coen-Cagli, R., Kanitscheider, I. & Pouget, A. Correlations and neuronal population information. *Annu. Rev. Neurosci.* **39**, 237–256 (2016).

[14] Panzeri, S., Moroni, M., Safaai, H. & Harvey, C. D. The structures and functions of correlations in neural population codes. *Nat. Rev. Neurosci.* **23**, 551–567 (2022).

[15] Bartolo, R., Saunders, R. C., Mitz, A. R. & Averbeck, B. B. Information-limiting correlations in large neural populations. *J Neurosci.* **40**, 1668–1678 (2020).

[16] Rumyantsev, O. I. *et al.* Fundamental bounds on the fidelity of sensory cortical coding. *Nature* **580**, 100–105 (2020).

[17] Kafashan, M. *et al.* Scaling of sensory information in large neural populations shows signatures of information-limiting correlations. *Nat. Commun.* **12**, 473 (2021).

[18] Hazon, O. *et al.* Noise correlations in neural ensemble activity limit the accuracy of hippocampal spatial representations. *Nat. Commun.* **13**, 4276 (2022).

[19] Abbott, L. F. & Dayan, P. The effect of correlated variability on the accuracy of a population code. *Neural Comput.* **11**, 91–101 (1999).

[20] Sompolinsky, H., Yoon, H., Kang, K. & Shamir, M. Population coding in neuronal systems with correlated noise. *Phys. Rev. E* **64**, 051904 (2001).

[21] Moreno-Bote, R. *et al.* Information-limiting correlations. *Nat. Neurosci.* **17**, 1410–1417 (2014).

[22] Stringer, C., Michaelos, M., Tsyboulski, D., Lindo, S. E. & Pachitariu, M. High-precision coding in visual cortex. *Cell* **184**, 2767–2778 (2021).

[23] Ecker, A. S., Berens, P., Tolias, A. S. & Bethge, M. The effect of noise correlations in populations of diversely tuned neurons. *J Neurosci.* **31**, 14272–14283 (2011).

[24] Kanitscheider, I., Coen-Cagli, R. & Pouget, A. Origin of information-limiting noise correlations. *Proc. Natl. Acad. Sci. U.S.A.* **112**, E6973–E6982 (2015).

[25] Leavitt, M. L., Pieper, F., Sachs, A. J. & Martinez-Trujillo, J. C. Correlated variability modifies working memory fidelity in primate prefrontal neuronal ensembles. *Proc. Natl. Acad. Sci. U.S.A.* **114**, E2494–E2503 (2017).

[26] Safaai, H., von Heimendahl, M., Sorando, J. M., Diamond, M. E. & Maravall, M. Coordinated population activity underlying texture discrimination in rat barrel cortex. *J Neurosci.* **33**, 5843–5855 (2013).

[27] Insanally, M. N. *et al.* Spike-timing-dependent ensemble encoding by non-classically responsive cortical neurons. *Elife* **8**, e42409 (2019).

[28] Zylberberg, J. The role of untuned neurons in sensory information coding. *bioRxiv* 134379 (2017).

[29] Osako, Y. *et al.* Contribution of non-sensory neurons in visual cortical areas to visually guided decisions in the rat. *Curr. Biol.* **31**, 2757–2769 (2021).

[30] Montijn, J. S. *et al.* Strong information-limiting correlations in early visual areas. *bioRxiv* 842724 (2019).

[31] Zhang, W.-H., Wu, S., Josić, K. & Doiron, B. Sampling-based bayesian inference in recurrent circuits of stochastic spiking neurons. *Nat. Commun.* **14**, 7074 (2023).

[32] Camargo, S. *et al.* Scale-free correlations in the dynamics of a small (n 10000) cortical network. *Phys. Rev. E* **108**, 034302 (2023).

[33] Arieli, A., Sterkin, A., Grinvald, A. & Aertsen, A. Dynamics of ongoing activity: explanation of the large variability in evoked cortical responses. *Science* **273**, 1868–1871 (1996).

[34] Tsodyks, M., Kenet, T., Grinvald, A. & Arieli, A. Linking spontaneous activity of single cortical neurons and the underlying functional architecture. *Science* **286**, 1943–1946 (1999).

[35] Kenet, T., Bibitchkov, D., Tsodyks, M., Grinvald, A. & Arieli, A. Spontaneously emerging cortical representations of visual attributes. *Nature* **425**, 954–956 (2003).

[36] Luczak, A., Barthó, P. & Harris, K. D. Spontaneous events outline the realm of possible sensory responses in neocortical populations. *Neuron* **62**, 413–425 (2009).

[37] Berkes, P., Orbán, G., Lengyel, M. & Fiser, J. Spontaneous cortical activity reveals hallmarks of an optimal internal model of the environment. *Science* **331**, 83–87 (2011).

[38] Matsui, T. *et al.* Orthogonalization of spontaneous and stimulus-driven activity by hierarchical neocortical areal network in primates. *Nature Communications* **15**, 1–13 (2024).

[39] Minces, V., Pinto, L., Dan, Y. & Chiba, A. A. Cholinergic shaping of neural correlations. *Proc. Natl. Acad. Sci. U.S.A.* **114**, 5725–5730 (2017).

[40] Dadarlat, M. C. & Stryker, M. P. Locomotion enhances neural encoding of visual stimuli in mouse v1. *J Neurosci.* **37**, 3764–3775 (2017).

[41] Cohen, M. R. & Maunsell, J. H. Attention improves performance primarily by reducing interneuronal correlations. *Nat. Neurosci.* **12**, 1594–1600 (2009).

Supplementary Information

Population coding under the scale-invariance of high-dimensional noise

S. Amin Moosavi
Department of Neuroscience, Brown University, Providence, Rhode Island, USA

Sai Sumedh R. Hindupur
School of Engineering and Applied Sciences, Harvard University, Cambridge, Massachusetts, USA

Hideaki Shimazaki
Graduate School of Informatics, Kyoto University, Kyoto, Japan
Center for Human Nature, Artificial Intelligence, and Neuroscience (CHAIN), Hokkaido University, Sapporo, Japan

Table of Contents

Supplementary Note 1: Linear scaling of the total variance constrains the scaling of eigenvalues **2**

Supplementary Note 2: Scaling conditions for bounded and unbounded LFI **4**

Supplementary Note 3: Scaling of LFI under a scale-invariant eigenspectrum with a power-law relation to the angular occupation. **10**

Supplementary Note 4: Scale-invariant eigenspectrum under the linear scaling of the total variance **13**

Supplementary Note 5: Scale-invariance and LFI under an eigenvalue distribution having a finite mean **15**

Supplementary Note 6: LFI of the subsampled populations is a non-decreasing function of population size **17**

Supplementary Note 7: Noise of bounded subsampled populations contain differential correlations **19**

Supplementary Note 8: Noise of populations expressing finite limiting LFI may not contain differential correlations **22**

Supplementary Note 9: Differential correlations induce linearly scaling eigenvalues **25**

Supplementary Note 10: Subspace analysis by partial least squares may incorrectly report saturated LFI **27**

Supplementary Note 1: Linear scaling of the total variance constrains the scaling of eigenvalues

In this note, we discuss the linear scaling of the total variance in subsampled neurons, categorize the scaling behavior of eigenvalues, and outline constraints on eigenvalue scaling when the total variance scales linearly.

For any number of neurons N, the total variance V_N is equal to the sum of variances of individual neurons, which is also equal to the sum of all eigenvalues of the covariance matrix, i.e.,

$$V_N = \sum_{i=1}^{N} \sigma_{i,N}^2 = \sum_{i=1}^{N} \lambda_{i,N}, \tag{S2.1}$$

Here $\sigma_{i,N}$ is the standard deviation in the activity of neuron i in a subsampled population of size N. In a subsampled population of neurons, the variance of an individual neuron's activity is independent of the subpopulation size N, i.e., $\sigma_{i,N}^2 = \sigma_i^2$. We can consider a distribution of σ_i^2 across neurons with a positive mean μ_{σ^2} and a bounded support, i.e., the variance of a given neuron is non-negative by definition and cannot exceed an upper bound by physiological constraints. Looking at the variability in the activity of a randomly selected neuron in recordings of a neuronal population is equivalent to sampling σ_i^2 from its distribution. Therefore, for large enough N we have $V_N \approx N\mu_{\sigma_i^2}$. Because μ_σ is finite, we have

$$V_N \sim N. \tag{S2.2}$$

This adds important constraints on the scaling of the eigenvalues with respect to N.

To see this, we categorize the eigenvalues into those that scale linearly, sublinearly, and supra-linearly defined as follows. The set of indices corresponding to linearly scaling eigenvalues is defined as

$$L = \{j \in \{1, 2, \dots, N\} | \lambda_{j,N} = F_j(N) + b_j N\}, \tag{S2.3}$$

where $b_j > 0$ is a constant positive number, and $F_j(N)$ is a function satisfying

$$\lim_{N\to\infty} \frac{F_j(N)}{N} = 0. \tag{S2.4}$$

Here, we refer to $\lambda_j = F_j(N) + b_j N$ as linear eigenvalues because the linear term will dominate the behavior at large N. Next, we define a set of sublinear eigenvalues that grow slower than the linear function in the limit as

$$S_b = \{j \in \{1, 2, \dots, N\} | \lambda_{j,N} = G_j(N)\}, \tag{S2.5}$$

where $G_j(N)$ is a function satisfying

$$\lim_{N\to\infty} \frac{G_j(N)}{N} = 0. \tag{S2.6}$$

The sublinear eigenvalues can be a constant or a decreasing function of N. Similarly, we define a set of indices corresponding to supra-linear eigenvalues as

$$S_p = \{j \in \{1, 2, \dots, N\} | \lambda_{j,N} = H_j(N)\}, \tag{S2.7}$$

in which $H_j(N)$ is a function of N with the following property

$$\lim_{N\to\infty} \frac{H_j(N)}{N} = \infty. \tag{S2.8}$$

Given these definitions, an immediate consequence of the constraint given by Eq. S2.2 is that the supra-linear eigenvalues cannot exist under the linear scaling total variance. The second consequence is that the number of linear eigenvalues must converge to a fixed finite number as N increases. Otherwise, the sum of linearly increasing eigenvalues grows supra-linearly, which contradicts the linear increase in the total variance. For example, if the number of linear eigenvalues grows as N^ϕ, then the sum of all linear eigenvalues will scale as $N^{\phi+1}$ which is supralinear if $\phi > 0$. Then, the third consequence is that the number of elements (cardinality) in set S_b linearly increases with N.

In sum, at large N, the number of elements in set L approaches a constant integer $c > 0$, and consequently the number of elements in set S_b linearly increase with N, while the set S_p becomes empty, i.e.,

$$\lim_{N\to\infty} |L| = c, \quad \lim_{N\to\infty} |S_b| = \infty. \ , \quad \lim_{N\to\infty} |S_p| = 0. \tag{S2.9}$$

Supplementary Note 2: Scaling conditions for bounded and unbounded LFI

In this note, we derive the necessary and sufficient conditions on the covariance matrix that limit information about a stimulus when the size of a neuronal population N increases, given that the covariance matrices exhibit the linear scaling of the total variance with respect to N.

Let $\mathbf{f}_N(s)$ be a N dimensional vector whose elements are mean activity or tuning functions $f_i(s)$ ($i = 1 \dots, N$) of individual neurons at a given stimulus s. Assuming that the covariance matrix of neuronal activity is invertible, the linear Fisher information (LFI) about the stimulus s can be written as:

$$I_N = \mathbf{f}'_N(s)^{\mathrm{T}} \mathbf{\Sigma}_N^{-1} \mathbf{f}'_N(s) \tag{S3.1}$$

where $\mathbf{f}'_N(s)$ is the N dimensional vector composed of the derivatives of tuning functions with respect to s, assuming that the tuning functions are differentiable, and $\mathbf{\Sigma}$ is the covariance matrix.

We denote the i-th eigenvalue of the covariance matrix $\mathbf{\Sigma}$ in the N dimensional space as $\lambda_{i,N}$. Here we index the eigenvalues in a descending order (from large to small): $\lambda_{1,N} \geq \lambda_{2,N} \geq \cdots \geq \lambda_{N,N}$. We write the covariance matrix in terms of its eigenvalues $\lambda_{i,N}$ and eigenvectors $\mathbf{u}_{i,N}$ as

$$\mathbf{\Sigma}_N = \sum_{i=1}^{N} \lambda_{i,N} \mathbf{u}_{i,N} \mathbf{u}_{i,N}^{\mathrm{T}}, \tag{S3.2}$$

where T is the transposition operator. We can also write $\mathbf{f}'_N(s)$ as a linear combination of eigenvectors of the covariance matrix as

$$\mathbf{f}'_N(s) = |\mathbf{f}'_N(s)| \sum_{i=1}^{N} \cos\theta_{i,N} \mathbf{u}_{i,N}, \tag{S3.3}$$

where $\theta_{i,N}$ is the angle between the vector $\mathbf{f}'_N(s)$ and the i-th eigenvector of the covariance matrix $\mathbf{u}_{i,N}$. Using the above equations, we can rewrite the LFI as

$$I_N = \sum_{i=1}^{N} \frac{|\mathbf{f}'_N(s)|^2}{\lambda_{i,N}} \cos^2\theta_{i,N}. \tag{S3.4}$$

Eq. S3.4 indicates that whether the LFI is limited or not depends on combination of the scaling of $|\mathbf{f}'_N(s)|^2$, the eigenvalue $\lambda_{i,N}$, and the angular occupation $\cos^2\theta_{i,N}$. Each obeys a certain constraint, resulting in a characteristic scaling structure.

First, $|\mathbf{f}'_N(s)|^2$ is expected to scale with N

$$|\mathbf{f}'_N(s)|^2 \sim N. \tag{S3.5}$$

as long as each element $f'_i(s)^2$ is independently sampled from a distribution having a finite mean η because $E|\mathbf{f}'_N(s)|^2 = E\sum_i f_i(s)'^2 = N\eta$.

Second, the angular occupation is constrained by

$$\sum_{i=1}^{N} \cos^2\theta_{j,N} = 1. \tag{S3.6}$$

We will explain consequences of this constraint on angular occupation at the end of this section.

Third, the total sum of eigenvalues for the subsampled population scales linearly:

$$\sum_{i=1}^{N} \lambda_{i,N} \sim N \tag{S3.7}$$

As discussed in Supplementary Note 1, this constraint regulates the number of linear eigenvalues $|L|$ and sublinear eigenvalues $|S_b|$ in the large N limit while prohibiting the supralinear eigenvalues.

The LFI based on the above definitions can be written in terms of the contributions of the two defined sets as

$$\begin{aligned} I_N &= |\mathbf{f}'_N(s)|^2 \sum_{i=1}^{N} \frac{\cos^2\theta_{i,N}}{\lambda_{i,N}} \\ &= \sum_{i\in L} \frac{AN\cos^2\theta_{i,N}}{\lambda_{i,N}} + \sum_{i\in S_b} \frac{AN\cos^2\theta_{i,N}}{\lambda_{i,N}}. \end{aligned} \tag{S3.8}$$

where we used $|\mathbf{f}'_N(s)|^2 = AN$. For future reference, we define

$$W_L(N) = \sum_{j\in L} \cos^2\theta_{j,N}, \quad W_{S_b}(N) = \sum_{j\in S_b} \cos^2\theta_{j,N}, \tag{S3.9}$$

as the total angular occupation by these two sets.

To have bounded LFI, we expect that both of the two summation terms on the right-hand side of Eq. S3.8 converge to constant values as N increases. Here, we study the two terms.

Using $\cos^2\theta_{i,N} \leq 1$, the first term is bounded as

$$I_L(N) = \sum_{i\in L} \frac{A\cos^2\theta_{i,N}}{\frac{F_i(N)}{N} + b_i} \leq \sum_{i\in L} \frac{A}{\frac{F_i(N)}{N} + b_i}. \tag{S3.10}$$

Hence, applying the definition of the sublinear function (Eq. S2.4), individual terms in the summation in the r.h.s of the equation above approaches a finite value in the large N limit. Since the number of the linear eigenvalues $|L|$ is finite, their sum is finite. Therefore, the limit of $I_L(N)$ is finite, regardless of the behavior of $\cos^2\theta_{i,N}$ as a function of N.

The second term on the right-hand side of Eq. S3.8 is

$$I_{S_b}(N) = A\sum_{i\in S_b} \cos^2\theta_{i,N}\frac{N}{\lambda_{i,N}}, \tag{S3.11}$$

where $\lambda_{i,N} = G_i(N)$. Based on the definition of S_b, $N/\lambda_{i,N}$ in the above summation are unbounded functions of N. Therefore, to have an upper bound for $I_{S_b}(N)$, it is necessary that for all terms in this summation, $\cos^2\theta_{i,N}$ become decreasing functions of N faster than $\lambda_{i,N}/N$. Not only that, it must also be fast enough so that the summation converges to some constant value. In other words, to have an upper bound on $I_{S_b}(N)$, the minimum possible speed of decrease in $\cos^2\theta_{i,N}$ ($\forall i \in S_b$) as a function of N depend not only on the behavior of $\lambda_{i,N}/N$ but also on the number of terms in the summation, i.e. the number of elements in S_b. Note that the number of sublinear noise components generally increases with N.

Accordingly, the following two conditions comprise the necessary and sufficient conditions for bounded information. First, $W_{S_b}(N) = 0$ is sufficient for information to be bounded. Second, if $W_{S_b}(N) > 0$, the second term can be written as

$$I_{S_b}(N) = W_{S_b}(N)\sum_{i\in S_b} \pi_i \frac{AN}{\lambda_{i,N}}, \tag{S3.12}$$

where

$$\pi_i = \frac{\cos^2\theta_{i,N}}{W_{S_b}(N)}, \quad \sum_{i\in S_b}\pi_i = 1 \tag{S3.13}$$

forms the probability mass function. Therefore, the summation term in Eq. S3.12 is the expectation of unbounded functions $AN/\lambda_{i,N}$ that itself is unbounded. Below, we write this expectation by $\langle\cdot\rangle$. Thus the necessary and sufficient condition that $I_{S_b}(N)$ (as well as I_N) is bounded is

$$\lim_{N\to\infty} \frac{W_{S_b}(N)}{\langle N/\lambda_{i,N}\rangle^{-1}} = const. \tag{S3.14}$$

Note that due to the definition of the sublinear eigenvalues, $\langle N/\lambda_{i,N}\rangle^{-1}$ is a decreasing function that converges to zero in the limit. Thus, $W_{S_b}(N)$ must converge to zero equal to or faster than $\langle N/\lambda_{i,N}\rangle^{-1}$.

In summary, the necessary and sufficient condition that the information is bounded is that either $W_{S_b}(N) = 0$ or $W_{S_b}(N)$ converges to zero equal to or faster than $\langle N/\lambda_{i,N}\rangle^{-1}$. The necessary and sufficient condition for unbounded information is constructed similarly by negating the above conditions. The information is unbounded only if $W_{S_b}(N)$ converges slower than $\langle N/\lambda_{i,N}\rangle^{-1}$.

Necessary condition Consequently, the necessary condition for the bounded information is that $W_{S_b}(N)$ converges to zero, or alternatively $W_L(N)$ converges to one:

$$\lim_{N\to\infty} W_{S_b}(N) = 0 \text{ or } \lim_{N\to\infty} W_L(N) = 1. \tag{S3.15}$$

Further, one can consider a set that covers the linear eigenvalues and let the angular occupation by this set approach one to satisfy a necessary condition. We consider a positive integer $\kappa(N) \leq N$ such that a set of $i = 1, \dots, \kappa(N)$ includes all linear eigenvalues. We define their angular occupation as $W_\kappa(N) = \sum_{i=1}^{\kappa(N)} \cos^2\theta_{i,N}$. For the information to be bounded, it is necessary that $W_\kappa(N)$ converge to one:

$$\lim_{N\to\infty} W_\kappa(N) = 1 \tag{S3.16}$$

The correlations that violate this necessary condition result in unbounded information.

Sufficient conditions An exemplary sufficient condition for the bounded information is obtained as follows. Since $\lambda_{i,N} \geq \lambda_{N,N}$, we obtain the upper bound of $\langle N/\lambda_{i,N}\rangle$ replacing $\lambda_{i,N}$ ($i = 1, \dots, N-1$) with $\lambda_{N,N}$: $\langle N/\lambda_{i,N}\rangle \leq N/\lambda_{N,N}$. By multiplying $W_{S_b}(N) > 0$, we have the upper bound of $I_{S_b}(N)$

$$I_{S_b}(N) = W_{S_b}(N) \cdot \langle AN/\lambda_{i,N}\rangle \leq W_{S_b}(N) \cdot (AN/\lambda_{N,N}). \tag{S3.17}$$

Thus for the information to be bounded, it is sufficient if the upper bound approaches to a constant value as N goes to infinity:

$$\lim_{N\to\infty} \frac{W_{S_b}(N)}{\lambda_{N,N}/N} = const, \tag{S3.18}$$

where $\lim_{N\to\infty} \lambda_{N,N}/N = 0$ because of the definition of the sublinear function for $\lambda_{N,N}$. Consequently, the sufficient condition for the bounded information is that $W_{S_b}(N)$ approaches zero faster than $\lambda_{N,N}/N$. Further, one can consider a set that covers the sublinear eigenvalues and a faster decrease of their angular occupation than $\lambda_{N,N}/N$ as a sufficient condition.

Below, we present exemplary covariance matrices that bound and unbound the LFI, assuming specific scaling conditions for the eigenvalues and angular occupation (except for Example 1).

Example 1: Unbounded LFI If the eigenvalues of the covariance matrix are all sublinear functions, we have $W_{S_b} = 1$, which clearly violates the necessary condition. Thus, the LFI for such populations is unbounded.

Example 2: Bounded/unbounded LFI We consider only one sublinear ($i = N$) eigenvalue has a finite cosine direction ($\cos^2\theta_{N,N} > 0$), while the rest of sublinear eigenvalues have no angular occupation ($\cos^2\theta_{i,N} = 0$ for $i \neq N$ and $i \in S_b$). The linear eigenvalues occupy the rest of angular occupation: $W_L = 1 - \cos^2\theta_{N,N}$. Then, for the LFI to be bounded, $W_{S_b} = \cos^2\theta_{N,N}$ must decrease equal to or faster than $\lambda_{N,N}/N$. If $\cos^2\theta_{N,N} = N^{-\delta}$ and $\lambda_{N,N} \sim N^\zeta$ ($\zeta < 1$), the exponent must satisfy $-\delta < \zeta - 1$, namely $\delta > 1 - \zeta$. Otherwise, if $\delta < 1 - \zeta$, the LFI is unbounded.

Example 3: Bounded/unbounded LFI We consider the first N_c eigenvalues to be linear, and the rest are sublinear eigenvalues given by $\lambda_{i,N} \sim N^\zeta$ with $\zeta \leq 0$ ($i = N_c + 1, \dots, N$). Note that $\zeta \leq 0$ is necessary for linearly scaling total variance. We then assign $\cos^2\theta_{i,N} = N^{-\delta}$ for $i = N_c + 1, \dots, N$. The angular occupation by sublinear eigenvalues is

$$W_{S_b} = \sum_{i=N_c+1}^{N} N^{-\delta} = (N - N_c)N^{-\delta} = (1 - N_c/N)N^{1-\delta} \sim N^{1-\delta}, \tag{S3.19}$$

from which we find δ must satisfy $\delta > 1$. For the LFI to be bounded, W_{S_b} must decay faster than $\langle N/\lambda_{i,N}\rangle^{-1} \sim N^{\zeta-1}$. Thus if $1 - \delta < \zeta - 1$, namely $\delta > 2 - \zeta$, the information is bounded. Otherwise, if $\delta < 2 - \zeta$, the LFI is unbounded.

Below, we present examples of the bounded and unbounded information constructed from the scale-invariant eigenspectrum given by Eqs. 3 and 4.

Example 4: Unbounded information under the scale-invariant eigenspectrum For the power-law eigenspectrum with the exponent smaller than -1, exhibiting the scale-invariance with $\alpha > 0$, linear eigenvalues appear in the spectrum. We need to consider a set with finite angular occupations that are associated with these linear eigenvalues to satisfy a necessary condition for the bounded LFI. The eigenvalue at an integer $i = N^\beta$ $(0 < \beta < 1)$ sublinearly scales as $\lambda_i \sim N^{1-\beta(1+\alpha)}$ (see below), hence the first N^β eigenvalues include all the linear eigenvalues (see below). Using this bound, the uniform angular occupation ($\cos^2\theta_{i,N} = 1/N$) results in

$$W_L(N) < \sum_{i=1}^{N^\beta} \cos^2\theta_{i,N} = \sum_{i=1}^{N^\beta} 1/N = N^{\beta-1} \to 0, \tag{S3.20}$$

which violates the necessary condition for any $\beta \in (0,1)$, from which we conclude that the LFI is unbounded if all eigenvectors have the same angles to $\mathbf{f}'_N(s)$.

One can confirm that the first N^β eigenvalues contain both linear and sublinear eigenvalues as follows. If we consider the first N^β eigenvalues with $0 < \beta < 1$, we have $x_i < N^\beta/N \to 0$ for $i \leq N^\beta$ in the large N limit. We can then use $\lambda_i \propto N^{-\alpha} x_i^{-1-\alpha}$. Using this approximation, we find that the eigenvalue with $i = N^\beta$ scales as $\lambda_i \sim N^{1-\beta(1+\alpha)}$, which is a sublinear function of N. Thus, the first N^β eigenvalues include both linear and sublinear eigenvalues.

Example 5: Bounded information under the scale-invariant eigenspectrum Under the the scale-invariant eigenspectrum, we have $\lambda_{N,N} \propto N^{-\alpha}$ for large N. Consequently, the sufficient condition for the bounded information is that $W_{S_b}(N)$ approaches zero faster than $N^{-(1+\alpha)}$. Further, one can consider a set that covers the sublinear eigenvalues and a faster decrease of their angular occupation than $\lambda_{N,N}/N$ as a sufficient condition. Such a set is obtained by considering the eigenvalue at $i = N_c$, where N_c is a fixed constant independently from N. Since $x_{N_c} = N_c/N \to 0$, the eigenvalue at $i = N_c$ is a linear eigenvalue, indicating that a set $i = N_c + 1, \ldots, N$ includes linear and sublinear eigenvalues. Let the angular occupation for $i = N_c + 1, \ldots, N$ is given by $\cos^2\theta_{i,N} = N^{-\delta}$. The rest is assigned to the first N_c components. Then

$$W_{S_b}(N) < \sum_{i=N_c+1}^{N} N^{-\delta} = (N - N_c)N^{-\delta} = (1 - N_c/N)N^{1-\delta} \sim N^{1-\delta}. \tag{S3.21}$$

Thus $W_{S_b}(N)$ decays faster than $N^{-(1+\alpha)}$ if $1 - \delta < -(1+\alpha)$, namely $\delta > 2 + \alpha$.

As seen in these examples, one can construct the populations with bounded and unbounded LFI by appropriately assigning the angular occupations $\cos^2\theta_{i,N}$ to eigenvectors associated with linear or sublinear eigenvalues. However, the assignment must be done by keeping the sum of the angular occupations one (Eq. S3.6). Here, we summarize its consequences, including the cases when the angular occupations scale with N.

1. Assuming monotonicity, the angular occupation, $\cos^2\theta_{i,N}$, must be either (i) a function of N approaching a non-zero constant equal to or less than one in the large N limit, or (ii) a decreasing function of N that vanishes to zero in the large N limit or a constant zero.
2. Let C be the set with the non-zero angular occupations in the large N limit:

$$C = \{j \in \{1, 2, \ldots, N\} | \lim_{N\to\infty} \cos^2\theta_{j,N} > 0\}. \tag{S3.22}$$

   The size (cardinality) of the set C, $|C|$, must be finite; otherwise, the summation exceeds one for large N. The angular occupations of the complement of C ($i \notin C$) are zeros or functions vanishing to zero in large N. The size of the complement of C increases proportionally to N.
3. We define the total angular occupation by the set C as

$$W_C(N) = \sum_{i\in C} \cos^2\theta_{i,N}. \tag{S3.23}$$

   If $W_C(N) < 1$ in the limit of N, the sum of the angular occupations by the complement of the set C ($i \notin C$) in the limit must be non-zero. Let the angular occupations for $i \notin C$ scale as

$\cos^2\theta_{i,N} \propto N^{-\delta_i}$. If all of these $\cos^2\theta_{i,N}$ ($i \notin C$) decrease faster than N^{-1} (i.e., $\delta_i > 1$ for all $i \notin C$), the sum of these angular occupations vanishes to zero for large N (note that their number is proportional to N). Therefore, the scaling of $\cos^2\theta_{i,N}$ for all $i \notin C$ decreasing faster than N^{-1} is prohibited. Instead, there must be δ_i that satisfy $0 < \delta_i \leq 1$. The number of the set having this scaling must not increase faster than N^{δ_i}; The faster increase than N^{δ_i} results in the explosion of the summed angular occupation.

4. To the contrary, if $W_C(N)$ approaches one for large N, the angular occupations by the complement of the set C must vanish in large N. Therefore, if they scale, they must scale with either $\cos^2\theta_{i,N} \propto N^{-\delta_i}$ ($\delta_i > 1$) if its size is proportional to N or $\cos^2\theta_{i,N} \propto N^{-\delta_i}$ ($0 < \delta_i \leq 1$) with its size increasing slower than N^{δ_i}.

These consequences can be utilized to set a range of scaling parameters for the angular occupations when constructing populations with the bounded and unbounded LFI. For example, for the LFI to be bounded, the non-zero angular occupations must be assigned to linear eigenvalues, and their sum, $W_C(N)$, must converge to one to satisfy the necessary condition (Eq. S3.15). The consequence of this condition is written in the item #4, where the decreasing angular occupations must scale with $\cos^2\theta_{i,N} \propto N^{-\delta_i}$ ($\delta_i > 1$) if their number increases with N. In Example 3, we assigned the decreasing angular occupations ($\cos^2\theta_{i,N} = N^{-\delta}$) to the set of sublinear eigenvalues $i = N_c+1, \ldots, N$, whose number increases linearly. In this case, the decreasing angular occupations must scale with $\delta > 1$, allowing us to set the range of the parameter δ. Note that this is a consequence of the necessary condition for bounded LFI under Eq. S3.6. The LFI is bounded only if the angular occupations decrease much faster.

Interestingly, if C is an empty set, namely if all $\cos^2\theta_{i,N}$ are decreasing functions of N that vanish to zero or constant zeros, the LFI is unbounded regardless of the composition of the eigenspectrum. Since the number of linear eigenvalues is at most finite under the linear scaling of the total variance, the sum of their angular occupations diminishes to zero, which violates the necessary condition (Eq. S3.15) for the bounded LFI. The situation applies to, but is not limited to, the covariance matrices obtained by shuffling the trials. The shuffling destroys the directional information of eigenvectors toward a signal and assigns the angular occupations uniformly, resulting in $\cos^2\theta_{i,N} \propto N^{-1}$ for all i.

Finally, we remark that the necessary and sufficient condition derived in this supplementary note was obtained under the constraint of the linear increase of the total variance for the noise covariance. The derivation also did not rely on the functional form of $\cos^2\theta_{i,N}$ with respect to N although we introduced scaling when we presented the examples and discussed the constraints on the angular occupations. The linear increase of the total variance is not a sufficient condition but a necessary condition for subsampled populations. In Supplementary Note 7, we show that the LFI of the subsampled populations is a non-decreasing function of N. In contrast, we note that the LFI of the populations subject to the constraint of the linear total variance can decrease with N. This is easily verified by the case with $W_L = 1$ while assuming the convergence of angular occupations: $\lim_{N\to\infty}\cos^2\theta_{i,N} = c_i (\geq 0)$. In this case, the LFI is identical to $I_L(N)$, which approaches:

$$I_L(N) = \sum_{i\in L} \frac{A\cos^2\theta_{i,N}}{\frac{F_i(N)}{N} + b_i} \to \sum_{i\in L} \frac{Ac_i}{b_i} \equiv I_L(\infty) \tag{S3.24}$$

If $F_i(N) > 0$ for all $i \in L$, $I_L(\infty)$ is an upper bound of LFI because

$$I_L(N) < \sum_{i\in L} \frac{A\cos^2\theta_{i,N}}{b_i} \to I_L(\infty), \tag{S3.25}$$

indicating that the LFI approaches the finite limiting constant $I_L(\infty)$ from the below. However, we note that $F_i(N)$ can be nonpositive: Since λ_i must be positive, we have $F_i(N) > -b_i N$, which means $F_i(N)$ can be a nonpositive value. When $0 > F_i(N) > -b_i N$ for $i \in L$, $I_L(\infty)$ is a lower bound of LFI: $\lim_{N\to\infty} I_L(N) < I_L(\infty)$, indicating that the LFI approaches $I_L(\infty)$ from the above. When $F_i(N) = 0$

for $i \in L$, the LFI is independent of N. Accordingly, the conditions for the boundedness derived in this note apply to the subsampled populations but are also applicable to the covariances of more general populations.

Supplementary Note 3: Scaling of LFI under a scale-invariant eigenspectrum with a power-law relation to the angular occupation.

Considering the scaling ansatz in Eqs. 3 and 4 with $\alpha > 0$ together with the following power-law relation (Eq. 5):

$$\cos^2\theta_i = \frac{\lambda_i^\gamma}{\sum_{i=1}^N \lambda_i^\gamma}, \tag{S4.1}$$

we can write the LFI as

$$I = |\mathbf{f}'_N(s)|^2 \frac{\sum \lambda_i^{\gamma-1}}{\sum \lambda_i^\gamma}. \tag{S4.2}$$

In this note, we establish analytical expression of the above LFI and prove that the information is a bounded function of N if

$$\gamma > \frac{2+\alpha}{1+\alpha}. \tag{S4.3}$$

Before proving the above statement, we argue, more generally, that regardless of the scaling of the eigenvalues, if $\gamma = 1$, we have

$$I = |\mathbf{f}'_N(s)|^2 \sum_{i=1}^N \frac{\cos^2\theta_i}{\lambda_i} = |\mathbf{f}'_N(s)|^2 \sum_{i=1}^N \frac{1}{\sum_{j=1}^N \lambda_j} = \frac{|\mathbf{f}'_N(s)|^2}{\sum_{j=1}^N \lambda_j} \sum_{i=1}^N 1 \sim N \tag{S4.4}$$

Therefore, for $\gamma = 1$, the information is a linearly increasing function of N. The last step is obtained by considering the fact that

$$|\mathbf{f}'_N(s)|^2 \sim N \quad \text{and} \quad \sum_{j=1}^N \lambda_j \sim N. \tag{S4.5}$$

See Supplementary Note 1 for more details. On the other hand, if $\gamma = 2$,

$$I = |\mathbf{f}'_N(s)|^2 \sum_{i=1}^N \frac{\cos^2\theta_i}{\lambda_i} = |\mathbf{f}'_N(s)|^2 \sum_{i=1}^N \frac{\lambda_i}{\sum_{j=1}^N \lambda_j^2} = \frac{|\mathbf{f}'_N(s)|^2 \sum_{i=1}^N \lambda_i}{\sum_{j=1}^N \lambda_j^2} \sim \frac{N^2}{N^2} \tag{S4.6}$$

that is a bounded function of N. It is clear that the numerator, which is a multiplication of the total variance with the norm of $\mathbf{f}'_N(s)$ scales as N^2. The denominator scaling, however, needs more attention. Since

$$\sum_{i=1}^N \lambda_i^2 < \left(\sum_{i=1}^N \lambda_i\right)^2 \sim N^2, \tag{S4.7}$$

we have $\left(\sum_{i=1}^N \lambda_i\right)^2$ as an upper bound of $\sum_{i=1}^N \lambda_i^2$. In addition, if there exists at least one eigenvalue that is a linearly increasing function of N, say $\lambda_1 \sim N$, then we have

$$\sum_{i=1}^N \lambda_i^2 > \lambda_1^2 \sim N^2 \tag{S4.8}$$

that specifies a lower bound for $\sum_{i=1}^N \lambda_i^2$; as a result, because both the upper and lower bounds scale with N^2, we can conclude that

$$\sum_{i=1}^N \lambda_i^2 \sim N^2. \tag{S4.9}$$

Up to this point, we showed that for $\gamma = 1$ the information is unbounded and for $\gamma = 2$ it is bounded. An immediate conclusion is that there must exist a $1 < \gamma < 2$ at which we have a transition from unbounded to bounded information. In the rest of this section, we prove that the critical value of $\gamma = \gamma_c$ at which the transition happens is identified by the following exponent relation:

$$\gamma_c = \frac{2+\alpha}{1+\alpha}. \tag{S4.10}$$

To prove that, we first focus on the scaling of

$$\Lambda(\phi) = \sum_{i=1}^N \lambda_i^\phi \tag{S4.11}$$

in which ϕ is a positive exponent. Considering the scaling ansatz (Eq. 3), we can write

$$\Lambda(\phi) = N^{-\alpha\phi} \sum_{i=1}^{N} g^{\phi}(x_i). \tag{S4.12}$$

Using the integral approximation of the summation, we have

$$\Lambda(\phi) \approx N^{1-\alpha\phi} \int_{1/N}^{1} g^{\phi}(x)dx = N^{1-\alpha\phi} \left[\int_{1/N}^{x_0} g^{\phi}(x)dx + \int_{x_0}^{1} g^{\phi}(x)dx \right], \tag{S4.13}$$

in which x_0 is a fixed small number ($1/N < x_0 \ll 1$) for which we can approximate

$$g(x) \approx b\mathrm{e}^{c} x^{-1-\alpha}. \tag{S4.14}$$

In Eq. S4.13, the second integral in the brackets is independent of N, and the first integral can be approximated as

$$\int_{1/N}^{x_0} g^{\phi}(x)\mathrm{d}x \approx \int_{1/N}^{x_0} b^{\phi}\mathrm{e}^{c\phi} x^{-\phi(1+\alpha)}\mathrm{d}x. \tag{S4.15}$$

By direct integration and replacing in Eq. S4.13 we get

$$\Lambda(\phi) \sim \begin{cases} N^{\phi} & \phi > 1/(1+\alpha), \\ N^{\phi}\log N & \phi = 1/(1+\alpha), \\ N^{1-\alpha\phi} & \phi < 1/(1+\alpha). \end{cases} \tag{S4.16}$$

See below for the derivations.

Using Eqs. S4.2 and S4.16, we can rewrite the LFI in terms of the function $\Lambda(\gamma)$ and $\Lambda(\gamma-1)$ as

$$I = |\mathbf{f}'_N(s)|^2 \frac{\Lambda(\gamma-1)}{\Lambda(\gamma)} \sim N^{1-\gamma}\Lambda(\gamma-1). \tag{S4.17}$$

because $\Lambda(\gamma) \sim N^{\gamma}$ for $\gamma > 1$. Using Eq. S4.16, we can write

$$I \sim \begin{cases} N^{0} & \gamma > (2+\alpha)/(1+\alpha), \\ \log N & \gamma = (2+\alpha)/(1+\alpha), \\ N^{2-\alpha(\gamma-1)-\gamma} & 1 < \gamma < (2+\alpha)/(1+\alpha). \end{cases} \tag{S4.18}$$

That is an unbounded function of N for $1 < \gamma \leq (2+\alpha)/(1+\alpha)$ and bounded for $\gamma > (2+\alpha)/(1+\alpha)$.

Finally, we note that $\cos^2\theta_{i,N}$ is computed as

$$\cos^2\theta_{i,N} \sim \begin{cases} \left(\lambda_{i,N}/N\right)^{\gamma} & \gamma > 1/(1+\alpha), \\ (\log N)^{-1}\left(\lambda_{i,N}/N\right)^{\gamma} & \gamma = 1/(1+\alpha), \\ N^{-1}\left(N^{\alpha}\lambda_{i,N}\right)^{\gamma} & \gamma < 1/(1+\alpha). \end{cases} \tag{S4.19}$$

which exhibits the scale invariance except for $\gamma = 1/(1+\alpha)$:

$$\cos^2\theta_{\delta i,\delta N} \sim \begin{cases} \delta^{-\gamma(1+\alpha)}\cos^2\theta_{i,N} & \gamma > 1/(1+\alpha), \\ \delta^{-1}\cos^2\theta_{i,N} & \gamma < 1/(1+\alpha). \end{cases} \tag{S4.20}$$

Derivation of $\Lambda(\phi)$ is as follows:

Case of $\phi > 1/(1+\alpha)$:

$$\Lambda(\phi) \approx N^{1-\alpha\phi} \int_{1/N}^{1} g^{\phi}(x)dx = N^{1-\alpha\phi} \left[\int_{1/N}^{x_0} g^{\phi}(x)dx + \underbrace{\int_{x_0}^{1} g^{\phi}(x)dx}_{Q(x_0,\phi)} \right]. \tag{S4.21}$$

Using the approximation of $g(x)$ for small x, we have

$$\int_{1/N}^{x_0} g^{\phi}(x)\mathrm{d}x \approx b^{\phi}\mathrm{e}^{c\phi}\int_{1/N}^{x_0} x^{-\phi(1+\alpha)}\mathrm{d}x = \frac{b^{\phi}e^{c\phi}}{\phi(1+\alpha)-1}\left[N^{\phi(1+\alpha)-1} - x_0^{1-\phi(1+\alpha)}\right]. \tag{S4.22}$$

Replacing in Eq. S4.21, we get

$$\Lambda(\phi) \approx N^{1-\alpha\phi}\left[\frac{b^{\phi}e^{c\phi}}{\phi(1+\alpha)-1}\left(N^{\phi(1+\alpha)-1} - x_0^{1-\phi(1+\alpha)}\right) + Q(x_0,\phi)\right] \tag{S4.23}$$

$$= \frac{b^{\phi}e^{c\phi}}{\phi(1+\alpha)-1}N^{\phi} + N^{1-\alpha\phi}\left[Q(x_0,\phi) - \frac{b^{\phi}e^{c\phi}}{\phi(1+\alpha)-1}x_0^{1-\phi(1+\alpha)}\right]. \tag{S4.24}$$

Because $\phi > 1-\alpha\phi$, in the large N limit

$$\Lambda(\phi) \sim N^{\phi}. \tag{S4.25}$$

Case of $\phi = 1/(1+\alpha)$:

$$\Lambda(\phi) \approx N^{1-\alpha\phi}\int_{1/N}^{1} g^{\phi}(x)dx = N^{1-\alpha\phi}\left[\int_{1/N}^{x_0} g^{\phi}(x)dx + \underbrace{\int_{x_0}^{1} g^{\phi}(x)dx}_{Q(x_0,\phi)}\right]. \tag{S4.26}$$

Using the approximation of $g(x)$ for small x, we have

$$\int_{1/N}^{x_0} g^{\phi}(x)\mathrm{d}x \approx b^{\phi}\mathrm{e}^{c\phi}\int_{1/N}^{x_0} x^{-\phi(1+\alpha)}\mathrm{d}x = b^{\phi}\mathrm{e}^{c\phi}\int_{1/N}^{x_0} x^{-1}\mathrm{d}x = b^{\phi}e^{c\phi}\left[\log x_0 + \log N\right]. \tag{S4.27}$$

Replacing in Eq. S4.26, we get

$$\Lambda(\phi) \approx N^{1-\alpha\phi}\left[b^{\phi}e^{c\phi}\left(\log x_0 + \log N\right) + Q(x_0,\phi)\right] \tag{S4.28}$$

$$= N^{\phi}\left[b^{\phi}e^{c\phi}\left(\log x_0 + \log N\right) + Q(x_0,\phi)\right]. \tag{S4.29}$$

In the last step we used $1-\alpha\phi = \phi$. Therefore, in the large N limit

$$\Lambda(\phi) \sim N^{\phi}\log N. \tag{S4.30}$$

Case of $\phi < 1/(1+\alpha)$:

$$\Lambda(\phi) \approx N^{1-\alpha\phi}\int_{1/N}^{1} g^{\phi}(x)dx = N^{1-\alpha\phi}\left[\int_{1/N}^{x_0} g^{\phi}(x)dx + \underbrace{\int_{x_0}^{1} g^{\phi}(x)dx}_{Q(x_0,\phi)}\right]. \tag{S4.31}$$

Using the approximation of $g(x)$ for small x, we have

$$\int_{1/N}^{x_0} g^{\phi}(x)\mathrm{d}x \approx b^{\phi}\mathrm{e}^{c\phi}\int_{1/N}^{x_0} x^{-\phi(1+\alpha)}\mathrm{d}x = \frac{b^{\phi}e^{c\phi}}{1-\phi(1+\alpha)}\left[x_0^{1-\phi(1+\alpha)} - N^{\phi(1+\alpha)-1}\right]. \tag{S4.32}$$

Replacing in Eq. S4.31, we get

$$\Lambda(\phi) \approx N^{1-\alpha\phi}\left[\frac{b^{\phi}e^{c\phi}}{1-\phi(1+\alpha)}\left(x_0^{1-\phi(1+\alpha)} - N^{\phi(1+\alpha)-1}\right) + Q(x_0,\phi)\right] \tag{S4.33}$$

$$= \frac{-b^{\phi}e^{c\phi}}{1-\phi(1+\alpha)}N^{\phi} + N^{1-\alpha\phi}\left[Q(x_0,\phi) + \frac{b^{\phi}e^{c\phi}}{1-\phi(1+\alpha)}x_0^{1-\phi(1+\alpha)}\right]. \tag{S4.34}$$

Because $\phi < 1-\alpha\phi$, in the large N limit

$$\Lambda(\phi) \sim N^{1-\alpha\phi} \tag{S4.35}$$

Supplementary Note 4: Scale-invariant eigenspectrum under the linear scaling of the total variance

In this note, we clarify the relationship between the scale-invariance of the eigenspectrum, the exponent of the power-law spectrum, and the eigenvalue scaling under the linear scaling of the total variance.

We start by assuming that the eigenspectrum is written in the form:

$$\lambda_{i,N} = c(N)g(x_i), \tag{S5.1}$$

where $c(N)$ is the scaling factor depending on the population size N and $g(x_i)$ is the scale-free structure of the eigenspectrum on the normalized index, $x_i = i/N$.

As discussed in Supplementary Note 1, the subsampled populations satisfies the linearly scaling total variance:

$$V_N = \sum_{i=1}^{N} \lambda_{i,N} = c(N) \sum_{i=1}^{N} g(x_i) \sim N. \tag{S5.2}$$

Using the integral approximation, the above summation is approximated as

$$c(N) \sum_{i=1}^{N} g(x_i) = Nc(N) \sum_{i=1}^{N} g(x_i) \frac{1}{N} \approx Nc(N) \int_{1/N}^{1} g(x)\mathrm{d}x. \tag{S5.3}$$

Note that the bounds of the integral are chosen over the domain of function $g(x)$, which is $[1/N, 1]$. We break the above integral into two parts:

$$\int_{1/N}^{1} g(x)\mathrm{d}x = \int_{1/N}^{x_0} g(x)\mathrm{d}x + \int_{x_0}^{1} g(x)\mathrm{d}x. \tag{S5.4}$$

While the second integral on the r.h.s of the above equation is independent of N, the first integral depends on N.

Suppose that we have the power-law spectrum $g(x) \sim x^{-\mu}$ ($\mu > 0$) at the limit of early indices of the eigenspectrum ($x \ll 1$). Because the eigenvalues are ordered descendingly, the slope must be non-positive, imposing $\mu > 0$. If $\mu \neq 1$, the above integral is approximated as

$$\begin{aligned} \int_{1/N}^{x_0} g(x)\mathrm{d}x &\sim \int_{1/N}^{x_0} x^{-\mu}\mathrm{d}x \\ &= \left[\frac{1}{1-\mu} x^{1-\mu}\right]_{1/N}^{x_0} = \frac{1}{\mu - 1}\left(N^{\mu-1} - x_0^{1-\mu}\right). \end{aligned} \tag{S5.5}$$

Further, if $\mu > 1$, the above integral, Eq. S5.5, scales as $N^{\mu-1}$, resulting in

$$\int_{1/N}^{1} g(x)\mathrm{d}x \sim N^{\mu-1} \tag{S5.6}$$

From Eqs. S5.3 and S5.6, the total variance scales as $V_N \propto c(N)N^{\mu}$. The constraint of the linearly scaling total variance imposes $c(N) = N^{-\alpha}$ with $\alpha = \mu - 1$, resulting in the following scale invariance:

$$\lambda_{i,N} = N^{-\alpha} g(x_i). \tag{S5.7}$$

We thus observe that when $\mu > 1$ ($\alpha > 0$), the eigenspectrum for larger N exhibits a smaller magnitude if plotted using the normalized index. In this case, the eigenvalues at the early indices scale linearly, $\lambda_{i,N} \sim N^{\alpha}(i/N)^{-\mu} \sim N$. These linearly scaling noise components can potentially limit the LFI.

To the contrary, if $0 < \mu < 1$, the above integral, Eq. S5.5, converges to a positive constant. Then, the total variance scales as $V_N \sim Nc(N)$, making $c(N)$ constant under the linear-scaling total variance constraint. In this case, we have the following scale-invariant eigenspectrum:

$$\lambda_{i,N} \sim g(x_i), \tag{S5.8}$$

which can be also written in the form of Eq. S5.7 using $\alpha = 0$. The eigenvalues at the limit of early indices scale sublinearly, $\lambda_{i,N} \sim N^{\mu}$ for a fixed $i(\ll N)$. Since the eigenspectrum is constructed in descending order, the later eigenvalues can not exceed the earlier eigenvalues, from which we conclude that all of the eigenvalues are sublinear functions of N if $\alpha = 0$. Without the presence of the linear scaling eigenvalues, the LFI can not be limited (Supplementary Note 3). This result implies that when neural populations show scale-invariant eigenspectra with $\alpha = 0$ in their noise covariance, their LFI is unbounded as long as the signal magnitude ($|\mathbf{f}'|^2$) increases with N.

Finally, the critical exponent $\mu = 1$ results in $V_N \sim Nc(N)\log N$, resulting in $c(N) \sim (\log N)^{-1}$. It is a decreasing function of N for $N \geq 1$. The eigenvalues at early indices scale as $\lambda_{i,N} \sim N/\log N$.

In summary, if we observe a scale-invariant eigenspectrum with an exponent $\alpha > 0$ for large N, the exponent μ of the power-law scaling must be $1 + \alpha$ in the limit of early indices, and the leading eigenvalues scale linearly. On the contrary, if we observe a scale-invariant eigenspectrum with an exponent $\alpha = 0$, the exponent of the power-law scaling μ must be less than one, and all eigenvalues scale sublinearly. We note that the same constraints are obtained by imposing the distribution of the eigenvalues to have a finite expected value (Supplementary Note 5).

The results above are obtained under the limit of large N and do not imply that the eigenspectrum does not depend on finite N for $\mu < 1$. Indeed, for $\mu \neq 1$, under the ansatz of Eq. S5.1, the scaling factor must follow

$$c(N) = \frac{1}{\frac{1}{\mu-1}\left(N^{\mu-1} - x_0^{1-\mu}\right) + \int_{x_0}^{1} g(x)\mathrm{d}x}, \tag{S5.9}$$

which is an increasing and saturating function with respect to N if $\mu < 1$. Thus, when plotted using the normalized index, we observe a larger eigenspectrum for larger but finite N if $\mu < 1$ before it converges. This contrasts with the case of $\mu > 1$, where the eigenspectrum of larger N exhibits a smaller magnitude. Consequently, given a finite population size N, one can still discern $\alpha > 0$ from $\alpha = 0$ by checking if the magnitude of the eigenspectrum increases or decreases with the subpopulation size.

Supplementary Note 5: Scale-invariance and LFI under an eigenvalue distribution having a finite mean

In this note, we show that the relation between the scaling parameter α and the power-law exponent μ of the eigenvalue spectrum under the linear total variance is obtained by constraining the eigenvalue distribution to have a finite mean.

Let $\hat{F}_N(\lambda) = \frac{1}{N}\sum_{i=1}^{N} \mathbf{1}_{\lambda_i \le \lambda}$ be an emprical cumulative distribution function (CDF) of the eigenvalues. Here, $\mathbf{1}_{\lambda_i \le \lambda}$ is an indicator function that takes one if the condition of the subscript is satisfied. Let $x_i = i/N$ for $i = 1, \dots, N$ be the normalized index of the eigenvalue λ_i. Since we order the eigenvalue in descending order, it is related to the empirical CDF as

$$x_i = 1 - \hat{F}_N(\lambda_i) + \frac{1}{N}, \tag{S6.1}$$

We assume that $\hat{F}_N(\lambda_i)$ approaches $F(\lambda)$ in the large N limit, where λ is a non-negative real value. Then, the eigenvalue spectrum and the CDF $F(\lambda)$ of the eigenvalues are related as follows.

$$1 - x = F(\lambda), \tag{S6.2}$$

where we introduced $x \in (0, 1]$. Similarly, we assume that the empirical density of the eigenvalues $\hat{\rho}(\lambda) = \sum_{i=1}^{N} \delta(\lambda - \lambda_i)$ converges to a continuous density function $\rho(\lambda) = \frac{dF(\lambda)}{d\lambda}$.

Thus, under the scaling-invariant eigenspectrum satisfying

$$\lambda(x) = N^{-\alpha} g(x), \tag{S6.3}$$

the eigenvalue density is related to $g(x)$ via

$$\rho(\lambda) = \frac{dF(\lambda)}{d\lambda} = -\frac{dx}{d\lambda} = -\left(\frac{d\lambda}{dx}\right)^{-1} = -N^{\alpha}\left(\frac{dg(x)}{dx}\right)^{-1}. \tag{S6.4}$$

In the following, we assume the power-law for the eigenvalue spectrum at low indices: $g(x) = bx^{-\mu}$ for $x \ll 1$. Then, if $\mu \neq 1$, the eigenvalue density follows the power-law with exponent $1 + \frac{1}{\mu}$ at $x \ll 1$:

$$\rho(\lambda) \propto \lambda^{-\left(1+\frac{1}{\mu}\right)} \tag{S6.5}$$

This is because, from $\lambda = N^{-\alpha} b x^{-\mu}$, we have

$$x = g^{-1}(N^{\alpha}\lambda) = b^{\frac{1}{\mu}}(N^{\alpha}\lambda)^{-\frac{1}{\mu}}, \tag{S6.6}$$

hence

$$\frac{dg(x)}{dx} = -b\mu x^{-\mu-1} = -b^{-\frac{1}{\mu}}\mu(N^{\alpha}\lambda)^{1+\frac{1}{\mu}}. \tag{S6.7}$$

The constraint of the linear scaling of the total variance or the sum of eigenvalues translates into the condition that the eigenvalue distribution has a finite positive mean. More specifically, we note that the mean of the sampled eigenvalues is related to the eigenvalue spectrum as follows:

$$\lim_{N\to\infty} \int \hat{\rho}(\lambda)\lambda\, d\lambda = \lim_{N\to\infty} \int_{\lambda_N}^{\lambda_1} \rho(\lambda)\lambda\, d\lambda = \lim_{N\to\infty} \int_{\lambda_N}^{\lambda_1} \left(-\lambda \frac{dx}{d\lambda}\right) d\lambda = \lim_{N\to\infty} \int_{1/N}^{1} \lambda(x)\, dx. \tag{S6.8}$$

For $\mu \neq 1$ and $\alpha > 0$, the r.h.s. of the above equation is given as

$$\begin{aligned}
\int_{1/N}^{1} \lambda(x)\, dx &= \int_{1/N}^{x_0} N^{-\alpha} g(x) dx + \int_{x_0}^{1} N^{-\alpha} g(x)\, dx \\
&= \int_{1/N}^{x_0} N^{-\alpha} b x^{-\mu}\, dx + C \\
&= \frac{b}{1-\mu}[x_0^{1-\mu} N^{-\alpha} - N^{\mu-1-\alpha}] + CN^{-\alpha},
\end{aligned} \tag{S6.9}$$

where C is a constant value. Note that $N^{-\alpha} \to 0$ in the large N limit for $\alpha > 0$. Thus, for the above equation to be finite, we need to impose $\mu - 1 - \alpha = 0$, or $\mu = 1 + \alpha$. In this case, $\mu > 1$, which makes the integral positive finite.

For $\mu \neq 1$ and $\alpha = 0$, the r.h.s. of the above equation is given as

$$\begin{aligned}\int_{1/N}^{1} \lambda(x)\, dx &= \int_{1/N}^{x_0} g(x)\, dx + \int_{x_0}^{1} g(x) dx \\ &= \int_{1/N}^{x_0} b x^{-\mu}\, dx + C \\ &= \frac{b}{1-\mu}[x_0^{1-\mu} - N^{\mu-1}] + C. \end{aligned} \tag{S6.10}$$

For the above equation to be finite, μ must satisfy $\mu < 1$ so that $N^{\mu-1} \to 0$ in the large N limit. These results are consistent with the scaling relations obtained under the linear scaling of the total variance in Supplementary Note 4 (The case with $\mu = 1$ is similarly obtained).

Finally, we also note that the LFI can be computed using the distributions of $\lambda_{i,N}$ and $\cos^2\theta_{i,N}$ as follows:

$$\begin{aligned} I_N &= |\mathbf{f}'_N(s)|^2 \sum_{i=1}^{N} \frac{\cos^2\theta_{i,N}}{\lambda_{i,N}} = AN^2 \frac{1}{N} \sum_{i=1}^{N} \frac{\cos^2\theta_{i,N}}{\lambda_{i,N}} \\ &\approx AN^2 \int p(\lambda, c) \frac{c}{\lambda}\, d\lambda\, dc \\ &= AN^2 \int \rho(\lambda) p(c|\lambda) \frac{c}{\lambda}\, d\lambda\, dc \\ &= AN^2 \int d\lambda \rho(\lambda) \frac{1}{\lambda} \int p(c|\lambda) c\, dc \end{aligned} \tag{S6.11}$$

Here we note that the power-law relation between the eigenvalue and angular occupation (Eq. 5 or Eq. S4.1) is defined as the conditional expectation of the angular occupation. Then, following the definition of $\Lambda(\gamma)$ in Supplementary Note 4, we obtain

$$\begin{aligned} I_N &= AN^2 \int d\lambda \rho(\lambda) \frac{1}{\lambda} \frac{\lambda^\gamma}{N \int \rho(\lambda) \lambda^\gamma d\lambda} \\ &= AN \frac{N \int \rho(\lambda) \lambda^{\gamma-1} d\lambda}{N \int \rho(\lambda) \lambda^\gamma d\lambda} \\ &= AN \frac{\Lambda(\gamma-1)}{\Lambda(\gamma)}, \end{aligned} \tag{S6.12}$$

which is equivalent to Eq. S4.17.

Supplementary Note 6: LFI of the subsampled populations is a non-decreasing function of population size

In this note, we derive a recurrence relation for the LFI of subsampled populations. This relation clarifies how the LFI changes when a neuron is added to a subpopulation, demonstrating that the LFI of subsampled populations is a non-decreasing function of population size.

When we increase the number of neurons by adding a neuron to an existing subpopulation of size N, the covariance of the larger population of size $N+1$, $\mathbf{\Sigma}_{N+1}$, contains the covariance of the population of size N, $\mathbf{\Sigma}_N$. Let Σ_{N+1} be the variance of the $(N+1)$-th neuron and $\mathbf{c}_N$ be the covariance between the existing N neurons and the $(N+1)$th neuron. The covariance matrix of the $N+1$ neurons is written as

$$\mathbf{\Sigma}_{N+1} = \begin{bmatrix} \mathbf{\Sigma}_N & \mathbf{c}_N \\ \mathbf{c}_N^{\mathrm{T}} & \Sigma_{N+1} \end{bmatrix}. \tag{S7.1}$$

The determinant of the sub-matrix $\mathbf{\Sigma}_N$ is the leading principle minor of the order N of the matrix $\mathbf{\Sigma}_{N+1}$. Further, the determinants of $\Sigma_1, \mathbf{\Sigma}_2, \ldots, \mathbf{\Sigma}_N, \mathbf{\Sigma}_{N+1}$ constitute the leading principle minors of $\mathbf{\Sigma}_{N+1}$. Sylvester's criterion states that $\mathbf{\Sigma}_{N+1}$ is positive definite only if all of the leading principal minors are positive.

From the block determinant formula, we have

$$\det \mathbf{\Sigma}_{N+1} = \det \mathbf{\Sigma}_N \left(\Sigma_{N+1} - \mathbf{c}_N^{\mathrm{T}} \mathbf{\Sigma}_N^{-1} \mathbf{c}_N \right) \tag{S7.2}$$

Given that $\mathbf{\Sigma}_N$ is positive definite, we have $\det \mathbf{\Sigma}_N > 0$. Then, $\mathbf{\Sigma}_{N+1}$ is positive definite only if

$$\omega_{N+1} \equiv \Sigma_{N+1} - \mathbf{c}_N^{\mathrm{T}} \mathbf{\Sigma}_N^{-1} \mathbf{c}_N > 0 \tag{S7.3}$$

Starting from a single neuron with a positive variance Σ_1, Sylvester's criterion is satisfied if we construct the covariance matrix recursively while satisfying $\omega_{N+1} > 0$. Indeed, this equation must be satisfied for a subsampled population of any size because the covariance of the subsampled population is positive definite.

We now consider the relation between the LFI of the population with size N and $N+1$. First, we calculate the inverse of the covariance matrix. Using the following formula for the inversion of a block matrix

$$\begin{bmatrix} \mathbf{A} & \mathbf{B} \\ \mathbf{C} & \mathbf{D} \end{bmatrix}^{-1} = \begin{bmatrix} \mathbf{A}^{-1} + \mathbf{A}^{-1}\mathbf{B}\left(\mathbf{D} - \mathbf{C}\mathbf{A}^{-1}\mathbf{B}\right)^{-1}\mathbf{C}\mathbf{A}^{-1} & -\mathbf{A}^{-1}\mathbf{B}\left(\mathbf{D} - \mathbf{C}\mathbf{A}^{-1}\mathbf{B}\right)^{-1} \\ -\left(\mathbf{D} - \mathbf{C}\mathbf{A}^{-1}\mathbf{B}\right)^{-1}\mathbf{C}\mathbf{A}^{-1} & \left(\mathbf{D} - \mathbf{C}\mathbf{A}^{-1}\mathbf{B}\right)^{-1} \end{bmatrix}, \tag{S7.4}$$

we obtain

$$\begin{aligned} \mathbf{\Sigma}_{N+1}^{-1} &= \begin{bmatrix} \mathbf{\Sigma}_N & \mathbf{c}_N \\ \mathbf{c}_N^{\mathrm{T}} & \Sigma_{N+1} \end{bmatrix}^{-1} \\ &= \begin{bmatrix} \mathbf{\Sigma}_N^{-1} + \mathbf{\Sigma}_N^{-1}\mathbf{c}_N \left(\Sigma_{N+1} - \mathbf{c}_N^{\mathrm{T}}\mathbf{\Sigma}_N^{-1}\mathbf{c}_N\right)^{-1}\mathbf{c}_N^{\mathrm{T}}\mathbf{\Sigma}_N^{-1} & -\mathbf{\Sigma}_N^{-1}\mathbf{c}_N \left(\Sigma_{N+1} - \mathbf{c}_N^{\mathrm{T}}\mathbf{\Sigma}_N^{-1}\mathbf{c}_N\right)^{-1} \\ -\left(\Sigma_{N+1} - \mathbf{c}_N^{\mathrm{T}}\mathbf{\Sigma}_{N-1}^{-1}\mathbf{c}_N\right)^{-1}\mathbf{c}_N^{\mathrm{T}}\mathbf{\Sigma}_N^{-1} & \left(\Sigma_{N+1} - \mathbf{c}_N^{\mathrm{T}}\mathbf{\Sigma}_N^{-1}\mathbf{c}_N\right)^{-1} \end{bmatrix}. \end{aligned} \tag{S7.5}$$

Using ω_{N+1} and

$$\mathbf{b}_N \equiv \mathbf{\Sigma}_N^{-1}\mathbf{c}_N, \tag{S7.6}$$

the inverse of the covariance matrix is written as

$$\mathbf{\Sigma}_{N+1}^{-1} = \begin{bmatrix} \mathbf{\Sigma}_N^{-1} + \omega_{N+1}^{-1}\mathbf{b}_N\mathbf{b}_N^{\mathrm{T}} & -\omega_{N+1}^{-1}\mathbf{b}_N \\ -\omega_{N+1}^{-1}\mathbf{b}_N^{\mathrm{T}} & \omega_{N+1}^{-1} \end{bmatrix}. \tag{S7.7}$$

Similarly to the covariance matrix, we separate $\mathbf{f}'_{N+1}(s)$ as

$$\mathbf{f}'_{N+1}(s) = \begin{bmatrix} \mathbf{f}'_N(s) \\ f'_{N+1}(s) \end{bmatrix}. \tag{S7.8}$$

With this, the LFI is obtained as

$$
\begin{aligned}
I_{N+1} &= \mathbf{f}'_{N+1}(s)^{\mathrm{T}}\mathbf{\Sigma}_{N+1}^{-1}\mathbf{f}'_{N+1}(s) \\
&= \mathbf{f}'_N(s)^{\mathrm{T}}\mathbf{\Sigma}_N^{-1}\mathbf{f}'_N(s) + \omega_{N+1}^{-1}\mathbf{f}'_N(s)^{\mathrm{T}}\mathbf{b}_N\mathbf{b}_N^{\mathrm{T}}\mathbf{f}'_N(s) - \omega_{N+1}^{-1}\mathbf{f}'_N(s)^{\mathrm{T}}\mathbf{b}_N f'_{N+1}(s) - \omega_{N+1}^{-1}f'_{N+1}(s)\mathbf{b}_N^{\mathrm{T}}\mathbf{f}'_N(s) + \omega_{N+1}^{-1}f'_{N+1}(s)^2 \\
&= \mathbf{f}'_N(s)^{\mathrm{T}}\mathbf{\Sigma}_N^{-1}\mathbf{f}'_N(s) + \omega_{N+1}^{-1}\left(\mathbf{f}'_N(s)^{\mathrm{T}}\mathbf{b}_N - f'_{N+1}(s)\right)^2
\end{aligned}
\tag{S7.9}
$$

from which we have

$$
I_{N+1} = I_N + \omega_{N+1}^{-1}\left(\mathbf{f}'_N(s)^{\mathrm{T}}\mathbf{\Sigma}_N^{-1}\mathbf{c}_N - f'_{N+1}(s)\right)^2. \tag{S7.10}
$$

Since $\omega_{N+1} > 0$, the second term of the above equation is nonnegative. Hence, we obtain

$$
I_{N+1} \geq I_N, \tag{S7.11}
$$

where the equality holds for $\mathbf{f}'_N(s)^{\mathrm{T}}\mathbf{\Sigma}_N^{-1}\mathbf{c}_N = f'_{N+1}(s)$. This proves that the LFI of the subsampled population is a non-decreasing function of N.

Eq. S7.10 provides insights into how the information increases or does not increase by adding a neuron. First, if $\mathbf{c}_N = \mathbf{0}$, namely, if an added neuron is independent of the other N neurons, the LFI increases with $\Sigma_{N+1}^{-1}f'^2_{N+1}$. Further, if $f'_{N+1} = 0$, namely, even if we add a neuron that is not sensitive to a stimulus, the LFI increases with $\mathbf{\Sigma}_N^{-1}\mathbf{c}$. Finally, the LFI does not increase if $\mathbf{f}'^{\mathrm{T}}_N\mathbf{\Sigma}_N^{-1}\mathbf{c}_N = f'_{N+1}$.

Note that the LFI can be interpreted as an infinitesimal value of the squared standardized mean difference along the direction that discriminates the distributions of the neural activity responding to two close stimulus conditions s and $s + ds$. If we have two multivariate distributions with mean $\mathbf{f}_N(s)$ and $\mathbf{f}_N(s + ds)$ and the same covariance matrix $\mathbf{\Sigma}_N$, the linear discriminant analysis tells that the direction $\mathbf{w}_N = \mathbf{\Sigma}_N^{-1}\delta\mathbf{f}_N(s)$, where $\delta\mathbf{f}_N(s) = \mathbf{f}_N(s+ds) - \mathbf{f}(s)$, best discriminates the stimuli. One can project the data on this line by $\mathbf{w}_N^{\mathrm{T}}\mathbf{x}$, resulting in uni-variate distributions with $\mathcal{N}(\mathbf{w}_N^{\mathrm{T}}\mathbf{f}_N(s), \mathbf{w}_N^{\mathrm{T}}\mathbf{\Sigma}_N\mathbf{w}_N)$ or $\mathcal{N}(\mathbf{w}_N^{\mathrm{T}}\mathbf{f}_N(s+ds), \mathbf{w}_N^{\mathrm{T}}\mathbf{\Sigma}_N\mathbf{w}_N)$, depending on the stimuli. The separability of these two distributions is quantified by the standardized mean difference,

$$
\frac{\mathbf{w}_N^{\mathrm{T}}\mathbf{f}_N(s+ds) - \mathbf{w}_N^{\mathrm{T}}\mathbf{f}_N(s)}{\sqrt{\mathbf{w}_N^{\mathrm{T}}\mathbf{\Sigma}_N\mathbf{w}_N}}, \tag{S7.12}
$$

and its square is given as

$$
\frac{\left(\mathbf{w}_N^{\mathrm{T}}\delta\mathbf{f}_N(s)\right)^2}{\mathbf{w}_N^{\mathrm{T}}\mathbf{\Sigma}_N\mathbf{w}_N} = \frac{\left(\delta\mathbf{f}_N(s)^{\mathrm{T}}\mathbf{\Sigma}_N^{-1}\delta\mathbf{f}_N(s)\right)^2}{\delta\mathbf{f}_N(s)^{\mathrm{T}}\mathbf{\Sigma}_N^{-1}\mathbf{\Sigma}_N\mathbf{\Sigma}_N^{-1}\delta\mathbf{f}_N(s)} = \delta\mathbf{f}_N(s)^{\mathrm{T}}\mathbf{\Sigma}_N^{-1}\delta\mathbf{f}_N(s) \simeq I_N(ds)^2. \tag{S7.13}
$$

Thus, $I_N = I_{N+1}$, namely $\mathbf{f}'_N(s)^{\mathrm{T}}\mathbf{\Sigma}_N^{-1}\mathbf{c}_N = f'_{N+1}$, is interpreted as the condition that does not change the ability to discriminate the two stimuli along the direction $\mathbf{w}_N$.

Supplementary Note 7: Noise of bounded subsampled populations contain differential correlations

In this note, we prove that the noise covariance of subsampled populations inducing saturating LFI can be decomposed into a covariance that induces unbounded LFI and differential correlations. This demonstrates that the boundedness of LFI under subsampling conditions is directly linked to the presence of differential correlations.

Given an (invertible) covariance matrix $\mathbf{\Sigma}_N^0$ whose LFI $I_0 = \mathbf{f}'_N(s)^{\mathrm{T}}(\mathbf{\Sigma}_N^0)^{-1}\mathbf{f}'_N(s)$ does not saturate as N goes infinity, Moreno-Bote et al. proved that the following specific form of correlations always limit the information[1]:

$$\mathbf{\Sigma}_N = \mathbf{\Sigma}_N^0 + \epsilon \mathbf{f}'_N(s)\mathbf{f}'_N(s)^{\mathrm{T}}, \tag{S8.1}$$

where $\epsilon \mathbf{f}'_N(s)\mathbf{f}'_N(s)^{\mathrm{T}}$ is called the differential correlations with ϵ being a non-zero constant. It can be confirmed as follows. Applying the Sherman–Morrison formula, the inverse of $\mathbf{\Sigma}$ is given as

$$\mathbf{\Sigma}_N^{-1} = (\mathbf{\Sigma}_N^0)^{-1} - \frac{\epsilon}{1+\epsilon I_0}(\mathbf{\Sigma}_N^0)^{-1}\mathbf{f}'_N(s)\mathbf{f}'_N(s)^{\mathrm{T}}(\mathbf{\Sigma}_N^0)^{-1}. \tag{S8.2}$$

Consequently, the LFI $I_N = \mathbf{f}'_N(s)^{\mathrm{T}}\mathbf{\Sigma}_N^{-1}\mathbf{f}'_N(s)$ follows

$$I_N = \frac{I_0}{1+\epsilon I_0}. \tag{S8.3}$$

Given that I_0 is a non-saturating function of N, the above equation is a saturating function that converges to $1/\epsilon$ as N goes infinity. Thus, the differential correlations make the information limited.

It was further demonstrated that the differential correlations are special because adding an outer product of any other direction to $\mathbf{\Sigma}_0$ can not limit the information. Therefore, they proposed that differential correlations are the only information-limiting correlations. The intuition behind this is that the noise structure $\epsilon \mathbf{f}'_N(s)\mathbf{f}'_N(s)^{\mathrm{T}}$ aligns with the direction of a signal change. No linear decoder can use such a structure to improve estimation accuracy. However, the proof is based on adding a rank-one matrix to $\mathbf{\Sigma}_0$. While they showed that among the rank-one matrix, only the differential correlation limits the LFI, the proof does not exclude the possibility that a more general covariance matrix that can not be written in the form of Eq. S8.1, i.e., addition of a matrix whose rank is higher than one or a matrix that can not be written as the addition of a matrix, such as a rotation of $\mathbf{\Sigma}_0$, limits the information.

Here, we remark that it is impossible to directly test the presence of differential correlations by using Eq. 9 because I_0 is an arbitrarily increasing unbounded function, and ϵ is unknown a priori. Namely, as I_0 at large N is constructed using the sublinear eigenvalues of $\mathbf{\Sigma}_N^0$ (Supplementary Note 2), its scaling arbitrarily depends on the scaling of these sublinear noise components. Accordingly, the LFI following Eq. 9 is an arbitrarily increasing and saturating function of N. Thus, one can not fit the empirical LFI to Eq. 10 to prove or disprove the presence of differential correlations.

We examine if the covariance matrix of subsampled populations resulting in saturation of the LFI contains the differential correlations. We start with the assumptions that the covariance matrix $\mathbf{\Sigma}_N$ for any finite N is positive definite and that $I_N = \mathbf{f}'_N(s)^{\mathrm{T}}\mathbf{\Sigma}_N^{-1}\mathbf{f}'_N(s)$ saturates in the limit of N: $I_N \to I_\infty$, where I_∞ is a finite value. One can formally test the presence of the differential correlations by examining if

$$\mathbf{\Sigma}_N^0 = \mathbf{\Sigma}_N - \epsilon \mathbf{f}'_N(s)\mathbf{f}'_N(s)^{\mathrm{T}}. \tag{S8.4}$$

is a (invertible) covariance matrix (i.e., a positive definite matrix). If $\mathbf{\Sigma}_N^0$ is invertible, using the Sherman-Morrison formula, the LFI $I_0 = \mathbf{f}'_N(s)^{\mathrm{T}}(\mathbf{\Sigma}_N^0)^{-1}\mathbf{f}'_N(s)$ is obtained as

$$I_0 = \frac{I_N}{1-\epsilon I_N} \tag{S8.5}$$

Consequently, we have

$$I_N = \frac{I_0}{1+\epsilon I_0}, \tag{S8.6}$$

from which we confirm that the saturating value of I_N is $1/\epsilon = I_\infty$. Further, I_0 is unbounded since it goes to infinity as I_N approaches $I_\infty = 1/\epsilon$ in the limit of N. Thus, the presence of differential correlations is guaranteed if $\mathbf{\Sigma}_N^0 = \mathbf{\Sigma}_N - \epsilon \mathbf{f}_N'(s)\mathbf{f}_N'(s)^{\mathrm{T}}$ is positive definite when we use $\epsilon = 1/I_\infty$. Note that this condition excludes the case $I_\infty = I_N$, namely, the LFI is constant irrespective of the population size. In this case, $\mathbf{\Sigma}_N^0$ is not invertible because $1 - \epsilon I_N = 0$. We thus restrict our analysis to the subsampled population that increases the LFI with N: $I_{N+1} > I_N$.

Given a positive definite covariance matrix $\mathbf{\Sigma}_{N+1}$, we ask if

$$\mathbf{\Sigma}_{N+1}^0 = \mathbf{\Sigma}_{N+1} - \epsilon \mathbf{f}_{N+1}'(s)\mathbf{f}_{N+1}'(s)^{\mathrm{T}} \tag{S8.7}$$

is positive definite or not. If so, $\mathbf{\Sigma}_{N+1}$ can be decomposed into a covariance matrix and differential correlations. Since we consider an incremental increase in the population size from N to $N+1$, it can be written as

$$\mathbf{\Sigma}_{N+1}^0 = \begin{bmatrix} \mathbf{\Sigma}_N - \epsilon \mathbf{f}_N'(s)\mathbf{f}_N'(s)^{\mathrm{T}} & \mathbf{c}_N - \epsilon \mathbf{f}_N'(s) f_{N+1}'(s) \\ \mathbf{c}_N^{\mathrm{T}} - \epsilon f_{N+1}'(s)\mathbf{f}_N'(s)^{\mathrm{T}} & \Sigma_{N+1} - \epsilon f_{N+1}'(s)^2 \end{bmatrix}. \tag{S8.8}$$

Note that the upper left block matrix is $\mathbf{\Sigma}_N^0$. Hence, by applying the block determinant formula, the determinant of $\mathbf{\Sigma}_{N+1}^0$ is given by

$$\det \mathbf{\Sigma}_{N+1}^0 = \det \mathbf{\Sigma}_N^0 + \Sigma_{N+1} - \epsilon f_{N+1}'(s)^2 - \left(\mathbf{c}_N - \epsilon f_{N+1}'(s)\mathbf{f}_N'(s)\right)^{\mathrm{T}} \left(\mathbf{\Sigma}_N^0\right)^{-1} \left(\mathbf{c}_N - \epsilon f_{N+1}'(s)\mathbf{f}_N'(s)\right). \tag{S8.9}$$

From this equation, the difference between the determinant of $\mathbf{\Sigma}_{N+1}^0$ and $\mathbf{\Sigma}_N^0$ is given as

$$\begin{aligned} &\det \mathbf{\Sigma}_{N+1}^0 - \det \mathbf{\Sigma}_N^0 && \text{(S8.10)} \\ &= \Sigma_{N+1} - \epsilon f_{N+1}'(s)^2 - \left(\mathbf{c}_N - \epsilon f_{N+1}'(s)\mathbf{f}_N'(s)\right)^{\mathrm{T}} \left(\mathbf{\Sigma}_N^0\right)^{-1} \left(\mathbf{c}_N - \epsilon f_{N+1}'(s)\mathbf{f}_N'(s)\right) \\ &= \Sigma_{N+1} - \epsilon f_{N+1}'(s)^2 \\ &\quad - \mathbf{c}_N^{\mathrm{T}} \left(\mathbf{\Sigma}_N^0\right)^{-1} \mathbf{c}_N + 2\mathbf{c}_N^{\mathrm{T}} \left(\mathbf{\Sigma}_N^0\right)^{-1} \epsilon f_{N+1}'(s)\mathbf{f}_N'(s) - \epsilon f_{N+1}'(s)\mathbf{f}_N'(s)^{\mathrm{T}} \left(\mathbf{\Sigma}_N^0\right)^{-1} \epsilon f_{N+1}'(s)\mathbf{f}_N'(s). && \text{(S8.11)} \end{aligned}$$

Using $I_c \equiv \mathbf{f}_N'(s)^{\mathrm{T}}\mathbf{\Sigma}_N^{-1}\mathbf{c}_N$, $I_N = \mathbf{f}_N'(s)^{\mathrm{T}}\mathbf{\Sigma}_N^{-1}\mathbf{f}_N'(s)$, and the Sherman-Morrison formula for $\mathbf{\Sigma}_N^0$,

$$\left(\mathbf{\Sigma}_N^0\right)^{-1} = \left(\mathbf{\Sigma}_N - \epsilon \mathbf{f}_N'(s)\mathbf{f}_N'(s)^{\mathrm{T}}\right)^{-1} = \mathbf{\Sigma}_N^{-1} + \frac{\epsilon \mathbf{\Sigma}_N^{-1}\mathbf{f}_N'(s)\mathbf{f}_N'(s)^{\mathrm{T}}\mathbf{\Sigma}_N^{-1}}{1 - \epsilon \mathbf{f}_N'(s)^{\mathrm{T}}\mathbf{\Sigma}_N^{-1}\mathbf{f}_N'(s)}, \tag{S8.12}$$

the above equation becomes

$$\begin{aligned} &\det \mathbf{\Sigma}_{N+1}^0 - \det \mathbf{\Sigma}_N^0 \\ &= \Sigma_{N+1} - \epsilon f_{N+1}'(s)^2 - \left(\mathbf{c}_N^{\mathrm{T}}\mathbf{\Sigma}_N^{-1}\mathbf{c}_N + \frac{\epsilon I_c^2}{1 - \epsilon I_N}\right) + 2\epsilon f_{N+1}'(s)\left(I_c + \frac{\epsilon I_c I_N}{1 - \epsilon I_N}\right) - \left(\epsilon f_{N+1}'(s)\right)^2 \left(I_N + \frac{\epsilon I_N^2}{1 - \epsilon I_N}\right) \\ &= \left(\Sigma_{N+1} - \mathbf{c}_N^{\mathrm{T}}\mathbf{\Sigma}_N^{-1}\mathbf{c}_N\right) - \frac{\epsilon I_c^2}{1 - \epsilon I_N} + 2\epsilon f_{N+1}'(s) I_c \left(1 + \frac{\epsilon I_N}{1 - \epsilon I_N}\right) - \epsilon f_{N+1}'(s)^2 - \left(\epsilon f_{N+1}'(s)\right)^2 I_N \left(1 + \frac{\epsilon I_N}{1 - \epsilon I_N}\right) \\ &= \left(\Sigma_{N+1} - \mathbf{c}_N^{\mathrm{T}}\mathbf{\Sigma}_N^{-1}\mathbf{c}_N\right) - \frac{\epsilon I_c^2}{1 - \epsilon I_N} + 2\epsilon f_{N+1}'(s)\frac{I_c}{1 - \epsilon I_N} - \epsilon f_{N+1}'(s)^2 - \left(\epsilon f_{N+1}'(s)\right)^2 \frac{I_N}{1 - \epsilon I_N} \\ &= \left(\Sigma_{N+1} - \mathbf{c}_N^{\mathrm{T}}\mathbf{\Sigma}_N^{-1}\mathbf{c}_N\right) - \frac{\epsilon I_c^2}{1 - \epsilon I_N} + 2\epsilon f_{N+1}'(s)\frac{I_c}{1 - \epsilon I_N} - \epsilon f_{N+1}'(s)^2 \left(1 + \frac{\epsilon I_N}{1 - \epsilon I_N}\right) \\ &= \left(\Sigma_{N+1} - \mathbf{c}_N^{\mathrm{T}}\mathbf{\Sigma}_N^{-1}\mathbf{c}_N\right) - \frac{\epsilon}{1 - \epsilon I_N}\left(I_c^2 - 2f_{N+1}'(s) I_c + f_{N+1}'(s)^2\right) \\ &= \left(\Sigma_{N+1} - \mathbf{c}_N^{\mathrm{T}}\mathbf{\Sigma}_N^{-1}\mathbf{c}_N\right) - \frac{\epsilon}{1 - \epsilon I_N}\left(I_c - f_{N+1}'(s)\right)^2. \end{aligned} \tag{S8.13}$$

Using S7.10, the equation above becomes

$$\begin{aligned} \det \mathbf{\Sigma}_{N+1}^0 - \det \mathbf{\Sigma}_N^0 &= \omega_{N+1} - \frac{\epsilon}{1 - \epsilon I_N}\left(\mathbf{f}_N'(s)^{\mathrm{T}}\mathbf{\Sigma}_N^{-1}\mathbf{c}_N - f_{N+1}'(s)\right)^2 \\ &= \omega_{N+1}\frac{\epsilon}{1 - \epsilon I_N}\left(\frac{1}{\epsilon} - I_N - \omega_{N+1}^{-1}\left(\mathbf{f}_N'(s)^{\mathrm{T}}\mathbf{\Sigma}_N^{-1}\mathbf{c}_N - f_{N+1}'(s)\right)^2\right) \\ &= \omega_{N+1}\frac{\epsilon}{1 - \epsilon I_N}\left(\frac{1}{\epsilon} - I_{N+1}\right) \\ &= \omega_{N+1}\frac{1 - \epsilon I_{N+1}}{1 - \epsilon I_N} \end{aligned} \tag{S8.14}$$

Note that $\omega_{N+1} > 0$ from Eq. S7.3. Furthermore, since $1/\epsilon = I_\infty$, and I_N is an increasing function of N ($I_\infty > I_{N+1} > I_N$), we can prove that this equation is positive for any finite N:

$$\det \mathbf{\Sigma}^0_{N+1} - \det \mathbf{\Sigma}^0_N = \omega_{N+1} \frac{I_\infty - I_{N+1}}{I_\infty - I_N} > 0. \tag{S8.15}$$

In summary, we showed

$$\det \mathbf{\Sigma}^0_{N+1} > \det \mathbf{\Sigma}^0_N. \tag{S8.16}$$

A single neuron ($N = 1$) with a positive variance Σ_1 satisfies $\det \Sigma^0_1 = \Sigma_1 - \epsilon f_1'(s)^2 > 0$ since $1/\epsilon > f_1'(s)^2 \Sigma_1^{-1} = I_1$. Thus, $\det \mathbf{\Sigma}^0_2 > 0$ for the population of two neurons. Then, according to Sylvester's criterion, $\mathbf{\Sigma}^0_2$ is positive definite. Recursively applying this relation to increasing the number of neurons up to $N+1$ guarantees that all of the leading principal minors of $\mathbf{\Sigma}^0_{N+1}$ is positive, proving that $\mathbf{\Sigma}^0_{N+1}$ is positive definite for any N.

References

[1] Moreno-Bote, R. *et al.* Information-limiting correlations. *Nat. Neurosci.* **17**, 1410–1417 (2014).

Supplementary Note 8: Noise of populations expressing finite limiting LFI may not contain differential correlations

In this note, we demonstrate that the differential correlations are not a unique form to represent information-limiting correlations for covariance matrices even if they are subject to the linearly increasing total variance. A specific decomposition of the covariance matrix $\mathbf{\Sigma}_N$ is shown below, which resembles the structure of differential correlations (having the sum of two matrices, one that limits information and the other that does not limit), but has a higher rank information-limiting matrix added to the non-information-limiting component. We then give a formal disproof.

Given that the linear and sublinear eigenvalues of $\mathbf{\Sigma}_N$ are respectively written as $\lambda_{i,N} = b_i N + F_i(N)$ ($i \in L$) and $\lambda_{i,N} = G_i(N)$ ($i \in S_b$) (See Supplementary Note 1), $\mathbf{\Sigma}_N$ can be in general decomposed as

$$\begin{aligned}\mathbf{\Sigma}_N &= \sum_{i\in L}[b_i N + F_i(N)]\mathbf{u}_{i,N}\mathbf{u}_{i,N}^T + \sum_{i\in S_b} G_i(N)\mathbf{u}_{i,N}\mathbf{u}_{i,N}^T \\ &= \left(\sum_{i\in L}\tilde{F}_i(N)\mathbf{u}_{i,N}\mathbf{u}_{i,N}^T + \sum_{i\in S_b} G_i(N)\mathbf{u}_{i,N}\mathbf{u}_{i,N}^T\right) + \sum_{i\in L}[b_i N + F_i(N) - \tilde{F}_i(N)]\mathbf{u}_{i,N}\mathbf{u}_{i,N}^T, \end{aligned} \tag{S9.1}$$

where $\tilde{F}_i(N)$ ($i \in L$) are arbitrary sublinear functions. Hence, we obtain the following expression for $\mathbf{\Sigma}_N$:

$$\mathbf{\Sigma}_N = \tilde{\mathbf{\Sigma}}_N^0 + \mathbf{\Sigma}_{\mathrm{IL}}, \tag{S9.2}$$

where the first term is

$$\begin{aligned}\tilde{\mathbf{\Sigma}}_N^0 &\equiv \sum_{i\in L}\tilde{F}_i(N)\mathbf{u}_{i,N}\mathbf{u}_{i,N}^T + \sum_{i\in S_b} G_i(N)\mathbf{u}_{i,N}\mathbf{u}_{i,N}^T \\ &= \sum_{i=1}^{N}\tilde{\lambda}_i\mathbf{u}_{i,N}\mathbf{u}_{i,N}^T. \end{aligned} \tag{S9.3}$$

Here we introduced $\tilde{\lambda}_i$ defined as $\tilde{\lambda}_i = \tilde{F}_i(N)$ if $i \in L$ and $\tilde{\lambda}_i = G_i(N)$ if $i \in S_b$. Note that we can choose $\tilde{F}_i(N)$ to be sublinear and non-negative: $\tilde{F}_i(N) > 0$ ($i \in S_b$). Then, $\tilde{\mathbf{\Sigma}}_N^0$ is a positive definite matrix. While $\tilde{\mathbf{\Sigma}}_N^0$ has the same set of eigenvectors as in $\mathbf{\Sigma}_N$, all of its eigenvalues are sublinear functions of N. Consequently, $\tilde{\mathbf{\Sigma}}_N^0$ results in unbounded LFI for any $\mathbf{f}'_N(s)$ (Supplementary Note 2). The second term is

$$\mathbf{\Sigma}_{\mathrm{IL}} \equiv \sum_{i\in L}(b_i N + F_i(N) - \tilde{F}_i(N))\mathbf{u}_{i,N}\mathbf{u}_{i,N}^T. \tag{S9.4}$$

which is a rank $|L|$ matrix. This decomposition is applicable to any covariance matrix, including the case that $\mathbf{f}'_N(s)$ and $\mathbf{\Sigma}_N$ result in the saturation of information. In this case, the covariance matrix $\mathbf{\Sigma}_N$ was expressed as the sum of two matrices, where $\tilde{\mathbf{\Sigma}}_N^0$ leads to unbounded LFI irrespective of the orientation of $\mathbf{f}'_N(s)$, and a rank $|L|$ matrix that is responsible for limiting the information. Note that this decomposition is not unique: We can construct various decompositions for any $\tilde{F}_i(N)$ as long as they are non-negative sublinear functions.

An example of decomposing a more specific covariance matrix disproves the presence of differential correlation in a covariance matrix subject to the linearly increasing total variance. Suppose that the kth eigenvector $\mathbf{u}_{k,N}$ ($k \in L$) of $\mathbf{\Sigma}_N$ perfectly aligns with the direction of $\mathbf{f}'_N(s)$. Such covariance matrix results in the bounded information because it satisfies the sufficient condition, $W_{S_b} = 0$ (Supplementary Note 2). Here, we note that, since $\mathbf{u}_{k,N} = \mathbf{f}'_N(s)/|\mathbf{f}'_N(s)|$, we have

$$\mathbf{u}_{k,N}\mathbf{u}_{k,N}^T = \frac{\mathbf{f}'_N(s)\mathbf{f}'_N(s)^T}{|\mathbf{f}'_N(s)|^2} = \frac{\mathbf{f}'_N(s)\mathbf{f}'_N(s)^T}{AN}. \tag{S9.5}$$

Using this relation, the covariance matrix is decomposed as

$$\begin{aligned}\mathbf{\Sigma}_N &= \sum_{i\in L}[b_i N + F_i(N)]\mathbf{u}_{i,N}\mathbf{u}_{i,N}^T + \sum_{i\in S_b} G_i(N)\mathbf{u}_{i,N}\mathbf{u}_{i,N}^T \\ &= \left(F_k(N)\mathbf{u}_{k,N}\mathbf{u}_{k,N}^T + \sum_{i\in L\backslash k}[b_i N + F_i(N)]\mathbf{u}_{i,N}\mathbf{u}_{i,N}^T + \sum_{i\in S_b} G_i(N)\mathbf{u}_{i,N}\mathbf{u}_{i,N}^T\right) + b_k N\mathbf{u}_{k,N}\mathbf{u}_{k,N}^T \\ &= \tilde{\mathbf{\Sigma}}_N^0 + \epsilon\mathbf{f}_N'(s)\mathbf{f}_N'(s)^T, \end{aligned} \tag{S9.6}$$

where we defined $\epsilon \equiv b_k/A$ and

$$\tilde{\mathbf{\Sigma}}_N^0 \equiv F_k(N)\mathbf{u}_{k,N}\mathbf{u}_{k,N}^T + \sum_{i\in L\backslash k}[b_i N + F_i(N)]\mathbf{u}_{i,N}\mathbf{u}_{i,N}^T + \sum_{i\in S_b} G_i(N)\mathbf{u}_{i,N}\mathbf{u}_{i,N}^T. \tag{S9.7}$$

If $F_k(N) > 0$, this matrix is positive definite. Unlike the previous decomposition, we did not exclude the linear eigenvalues except for k from $\tilde{\mathbf{\Sigma}}_N^0$. This is because $\mathbf{u}_{i,N}$ ($i \in L\backslash k$) are orthogonal to $\mathbf{f}_N'(s)$, therefore $\tilde{\mathbf{\Sigma}}_N^0$ still results in unbounded LFI (See also Supplementary Note 9). Thus, such a covariance $\mathbf{\Sigma}_N$ is written as a sum of a non-saturating (invertible) covariance matrix and the differential correlations. In other words, $\mathbf{\Sigma}_N$ contains the differential correlations.

However, $F_k(N)$ can be non-positive. The eigenvalues of $\mathbf{\Sigma}_N$, including the linear eigenvalues $\lambda_{i,N} = b_i N + F_i(N)$ ($i \in L$), must be positive so that $\mathbf{\Sigma}_N$ is positive definite. Hence, the sublinear functions $F_i(N)$ in the linear eigenvalues must satisfy $F_i(N) > -b_i N$, which allows $F_i(N)$ to be either zero or negative. If $F_k(N) \leq 0$, $\tilde{\mathbf{\Sigma}}_N^0$ is no longer a positive definite matrix. If $F_k(N) = 0$, i.e., $\lambda_{k,N} = b_k N$, the rank of $\tilde{\mathbf{\Sigma}}_N^0$ becomes $N-1$, and $\tilde{\mathbf{\Sigma}}_N^0$ is not invertible. The bounded covariance $\mathbf{\Sigma}_N$ having these properties can not be decomposed into a sum of a (invertible) covariance matrix and the differential correlations. This example disproves the statement that differential correlations are the only information-limiting correlations.

In what follows, we give a formal disproof of the differential correlations using the example above, following an approach that proved the presence of differential correlations for the subsampled populations with saturating LFI (Supplementary Note 7). We assume that we have $\mathbf{\Sigma}_N$ that results in the bounded information with its limit being given by $\lim_{N\to\infty} I_N = 1/\epsilon$, namely $\epsilon = 1/\lim_{N\to\infty} I_N$. The presence of the differential correlations is guaranteed if we can decompose $\mathbf{\Sigma}$ in the form of Eq. S8.1, where $\mathbf{\Sigma}_N^0$ is a positive definite covariance matrix.

Using eigenvectors of $\mathbf{\Sigma}_N$ and $\mathbf{f}_N'(s) = |\mathbf{f}_N'(s)|\sum_{i=1}^N \cos\theta_{i,N}\mathbf{u}_{i,N}$, $\mathbf{\Sigma}_N^0$ is written as

$$\begin{aligned}\mathbf{\Sigma}_N^0 &= \mathbf{\Sigma}_N - \epsilon\mathbf{f}_N'(s)\mathbf{f}_N'(s)^{\mathrm{T}} \\ &= \sum_{i=1}^N \lambda_{i,N}\mathbf{u}_{i,N}\mathbf{u}_{i,N}^{\mathrm{T}} - \epsilon AN\sum_{i,j}\cos(\theta_{i,N})\cos(\theta_{j,N})\mathbf{u}_{i,N}\mathbf{u}_j^{\mathrm{T}}\end{aligned}$$

A positive definite matrix $\mathbf{\Sigma}_N$ can be diagonalized by an orthogonal matrix as $\mathbf{\Sigma}_N = \mathbf{U}_N\mathbf{W}_N\mathbf{U}_N^{\mathrm{T}}$, where $\mathbf{W}_N$ is a diagonal matrix with its entries being the eigenvalues of $\mathbf{\Sigma}_N$. The ith elements of the jth column eigenvector $\mathbf{w}_{i,N}$ of $\mathbf{W}_N$ is given by a Kronecker delta $w_{ij,N} = \lambda_{i,N}\delta_{ij}$. Then from

$$\mathbf{\Sigma}_N^0 = \mathbf{U}_N(\mathbf{U}_N^{\mathrm{T}}\mathbf{\Sigma}_N^0\mathbf{U}_N)\mathbf{U}_N^{\mathrm{T}}, \tag{S9.8}$$

we investigate $\mathbf{W}_N^0 \equiv \mathbf{U}_N^{\mathrm{T}}\mathbf{\Sigma}_N^0\mathbf{U}_N$ because if $\mathbf{W}_N^0$ is a positive definite matrix, so is $\mathbf{\Sigma}_N^0$. Noting $\mathbf{U}_N\mathbf{W}_N = \mathbf{\Sigma}_N\mathbf{U}_N$ or $\mathbf{U}_N[\mathbf{w}_{1,1},\dots,\mathbf{w}_{1,N}] = \mathbf{\Sigma}_N[\mathbf{u}_{1,1},\dots,\mathbf{u}_{1,N}]$, we have $\mathbf{U}_N\mathbf{w}_{i,N} = \mathbf{\Sigma}_N\mathbf{u}_{i,N}$, from which we obtain

$$\mathbf{U}_N^{\mathrm{T}}\mathbf{u}_{i,N} = \mathbf{U}_N^{\mathrm{T}}\mathbf{\Sigma}_N^{-1}\mathbf{U}_N\mathbf{w}_{i,N} = \mathbf{W}_N^{-1}\mathbf{w}_{i,N} = \lambda_{i,N}^{-1}\mathbf{w}_{i,N}. \tag{S9.9}$$

Hence,

$$\begin{aligned}\mathbf{W}_N^0 &\equiv \mathbf{U}_N^{\mathrm{T}}\mathbf{\Sigma}_N^0\mathbf{U}_N \\ &= \sum_{i=1}^N \lambda_{i,N}\lambda_{i,N}^{-2}\mathbf{w}_{i,N}\mathbf{w}_{i,N}^{\mathrm{T}} - \epsilon N\sum_{i,j}\cos(\theta_{i,N})\cos(\theta_{j,N})\lambda_{i,N}^{-1}\lambda_{j,N}^{-1}\mathbf{w}_{i,N}\mathbf{w}_{j,N}^{\mathrm{T}}, \\ &= \sum_{i,j}^N\left(\delta_{ij}\lambda_{i,N}^{-1} - \epsilon N\cos(\theta_{i,N})\cos(\theta_{j,N})\lambda_{i,N}^{-1}\lambda_{j,N}^{-1}\right)\mathbf{w}_{i,N}\mathbf{w}_{j,N}^{\mathrm{T}}\end{aligned} \tag{S9.10}$$

The (k, l) element of $\mathbf{W}_N^0$ is computed as

$$
\begin{aligned}
[\mathbf{W}_N^0]_{kl} &= \sum_{i,j} \left(\delta_{ij} \lambda_{i,N}^{-1} - \epsilon AN \cos(\theta_{i,N}) \cos(\theta_{j,N}) \lambda_{i,N}^{-1} \lambda_{j,N}^{-1} \right) w_{ik,N} w_{jl,N} \\
&= \left(\delta_{kl} \lambda_{k,N}^{-1} - \epsilon AN \cos(\theta_{k,N}) \cos(\theta_{l,N}) \lambda_{i,N}^{-1} \lambda_{j,N}^{-1} \right) \lambda_{k,N} \lambda_{l,N} \\
&= \delta_{kl} \lambda_{k,N} - \epsilon AN \cos(\theta_{k,N}) \cos(\theta_{l,N}) \\
&= \begin{cases} \lambda_{k,N} - \epsilon AN \cos^2(\theta_{k,N}) & k = l \\ -\epsilon AN \cos(\theta_{k,N}) \cos(\theta_{l,N}) & k \neq l \end{cases}
\end{aligned}
\tag{S9.11}
$$

Hence, for $\mathbf{W}_N^0$ to be a positive definite matrix, it must satisfy

$$
\boldsymbol{v}_N^{\mathrm{T}} \mathbf{W}_N^0 \boldsymbol{v}_N = \sum_i \left(\lambda_{i,N} - \epsilon AN \cos^2(\theta_{i,N}) \right) v_{i,N}^2 - \epsilon AN \sum_{i \neq j} \cos(\theta_{i,N}) \cos(\theta_{j,N}) v_{i,N} v_{j,N} > 0 \tag{S9.12}
$$

for any non-zero real vector $\boldsymbol{v}_N$ ($\boldsymbol{v}_N \neq 0$) when $\epsilon = 1/I_\infty$.

We examine this condition with the simple case discussed above, in which one linear eigenvalue occupies a cosine direction to $\mathbf{f}'_N(s)$. For simplicity, we consider that the first linear eigenvalue occupies the cosine direction ($\cos^2 \theta_{1,N} = 1$). In this case,

$$
I = \sum_{i=1}^{N} \frac{|\mathbf{f}'_N(s)|^2 \cos^2 \theta_{i,N}}{\lambda_{i,N}}, = \frac{AN}{b_1 N + F_1(N)} \tag{S9.13}
$$

from which we obtain $I_\infty = A/b_1$. Hence we use $\epsilon = b_1/A$.

The quadratic term then becomes

$$
\begin{aligned}
\boldsymbol{v}_N^{\mathrm{T}} \mathbf{W}_N^0 \boldsymbol{v}_N &= (\lambda_{1,N} - \epsilon AN) v_{1,N}^2 + \sum_{i=2}^{N} \lambda_{i,N} v_{i,N}^2 \\
&= (F_1(N) + N(b_1 - \epsilon A)) v_{1,N}^2 + \sum_{i=2}^{N} \lambda_{i,N} v_{i,N}^2 \\
&= F_1(N) v_{1,N}^2 + \sum_{i=2}^{N} \lambda_{i,N} v_{i,N}^2,
\end{aligned}
\tag{S9.14}
$$

If $F_1(N) > 0$, $\mathbf{\Sigma}_N^0$ is positive definite. However, if $0 \geq F_1(N) > -b_1 N$, $\mathbf{\Sigma}_N^0$ is not positive definite. When $F_1(N) = 0$, $\mathbf{\Sigma}_N^0$ is not invertible, which also violates the condition for the differential correlations. We note that when $F_1(N) = \lambda_{1,N} - \epsilon AN < 0$, we have

$$
I = \frac{AN}{\lambda_{1,N}} > \frac{1}{\epsilon} = \frac{A}{b_1} = I_\infty \tag{S9.15}
$$

So the LFI is a decreasing function approaching I_∞.

With this example, we corroborated that if a linear eigenvalue of the covariance matrix occupies the angular occupation, and the sublinear component of the linear eigenvalue is not positive, the covariance matrix does not contain the differential correlations. In this case, the LFI is a decreasing function of N approaching to a finite value.

Supplementary Note 9: Differential correlations induce linearly scaling eigenvalues

In this note, we show that if $\mathbf{\Sigma}_N^0$ leads to the unbounded LFI for all directions of $\mathbf{f}'_N(s)$, by adding differential correlations, only one of the eigenvectors of $\mathbf{\Sigma}_N$ will be significantly aligned with $\mathbf{f}'_N(s)$ and only the eigenvalue associated with this eigenvector will linearly increase with N. Otherwise, if I_0 is unbounded only for specific stimuli, there are multiple linear eigenvalues in $\mathbf{\Sigma}_N$, that can span $\mathbf{f}'_N(s)$. These results show that aligning the linear eigenvalues with $\mathbf{f}'_N(s)$ is necessary to limit the information.

If differential correlations exist, for any subsample of neurons, $\mathbf{\Sigma}_N^0$ must exist and because it is a covariance matrix, it can be written in terms of its eigenvalues $\gamma_{i,N}$ and eigenvectors $\mathbf{v}_{i,N}$ as

$$\mathbf{\Sigma}_N^0 = \sum_{i=1}^{N} \gamma_{i,N} \mathbf{v}_{i,N} \mathbf{v}_{i,N}^{\mathrm{T}}. \tag{S10.1}$$

Since the set of orthonormal eigenvectors are a complete set, we can write $\mathbf{f}'_N(s)$ as a linear combination of the eigenvectors of $\mathbf{\Sigma}_N^0$:

$$\mathbf{f}'_N(s) = |\mathbf{f}'_N(s)| \sum_{i=1}^{N} \cos\phi_{i,N} \mathbf{v}_{k,N} \tag{S10.2}$$

with $\sum_i \cos^2\phi_{i,N} = 1$, in which $\phi_{i,N}$ is the angle between the i-th eigenvector of $\mathbf{\Sigma}_{0,N}$ and $\mathbf{f}'_N(s)$. We can also write

$$\begin{aligned}
\mathbf{\Sigma}_N =& \mathbf{\Sigma}_N^0 + \epsilon \mathbf{f}'_N(s)\mathbf{f}'_N(s)^{\mathrm{T}} \\
=& \sum_{i=1}^{N} \gamma_{i,N} \mathbf{v}_{i,N}\mathbf{v}_{i,N}^{\mathrm{T}} + \epsilon |\mathbf{f}'_N(s)|^2 \sum_{i=1}^{N}\sum_{j=1}^{N} \cos\phi_{i,N}\cos\phi_{j,N} \mathbf{v}_{i,N}\mathbf{v}_{j,N}^{\mathrm{T}} \\
=& \sum_{i=1}^{N}\sum_{j=1}^{N} (\delta_{ij}\gamma_{i,N} + \epsilon|\mathbf{f}'_N(s)|^2 \cos\phi_{i,N}\cos\phi_{j,N}) \mathbf{v}_{i,N}\mathbf{v}_{j,N}^{\mathrm{T}}.
\end{aligned} \tag{S10.3}$$

We multiply the above equation from the right side by $\mathbf{f}'_N(s)$

$$\begin{aligned}
\mathbf{\Sigma}_N \mathbf{f}'_N(s) =& |\mathbf{f}'_N(s)| \sum_{i=1}^{N}\sum_{j=1}^{N}\sum_{k=1}^{N} \cos\phi_{k,N} (\delta_{ij}\gamma_{i,N} + \epsilon|\mathbf{f}'_N(s)|^2 \cos\phi_{i,N}\cos\phi_{j,N}) \mathbf{v}_{i,N}\mathbf{v}_{j,N}^{\mathrm{T}}\mathbf{v}_{k,N} \\
=& |\mathbf{f}'_N(s)| \sum_{i=1}^{N}\sum_{j=1}^{N} \cos\phi_{j,N} (\delta_{ij}\gamma_{i,N} + \epsilon|\mathbf{f}'_N(s)|^2 \cos\phi_{i,N}\cos\phi_{j,N}) \mathbf{v}_{i,N} \\
=& |\mathbf{f}'_N(s)| \sum_{i=1}^{N} (\gamma_{i,N} + \epsilon|\mathbf{f}'_N(s)|^2) \cos\phi_{i,N} \mathbf{v}_{i,N}.
\end{aligned} \tag{S10.4}$$

Due to the fact that $I_0(N) = \mathbf{f}'_N(s)^{\mathrm{T}}(\mathbf{\Sigma}_N^0)^{-1}\mathbf{f}'_N(s)$ must be an unbounded function of N, there must be at least one non-zero $\cos\phi_{i,N}$ whose related eigenvalue is a sublinear function of N (Supplementary Note 2). Furthermore, if $\mathbf{\Sigma}_N^0$ is defined to be independent of $\mathbf{f}'_N(s)$ that is spanned by all of the eigenvectors of $\mathbf{\Sigma}_N^0$, and if information is limited for any $\mathbf{f}'_N(s)$, it is expected that all $\gamma_{i,N}$s are sublinear functions of N. Therefore, at large N limit, we have $\gamma_{i,N} \ll \epsilon|\mathbf{f}'_N(s)|^2$ for all $i = 1, \ldots, N$, and the above equation approaches to

$$\begin{aligned}
\lim_{N\to\infty} \mathbf{\Sigma}_N \mathbf{f}'_N(s) &= |\mathbf{f}'_N(s)| \sum_{i=1}^{N} (\epsilon|\mathbf{f}'_N(s)|^2) \cos\phi_{i,N} \mathbf{v}_{i,N} \\
&= (\epsilon|\mathbf{f}'_N(s)|^2)\mathbf{f}'_N(s).
\end{aligned} \tag{S10.5}$$

This result states that, in this limit, $\frac{\mathbf{f}'_N(s)}{|\mathbf{f}'_N(s)|}$ becomes an eigenvector of $\mathbf{\Sigma}_N$ with the eigenvalue of $\lambda = \epsilon|\mathbf{f}'_N(s)|^2$. In other words, $\mathbf{f}'_N(s)$ is spanned by only this specific eigenvector of $\mathbf{\Sigma}_N$. Namely, if the differential correlations exist in the neuronal data for all stimulus directions, we expect that only

one of the eigenvectors gets more significantly aligned with $\mathbf{f}'_N(s)$ as N increases. Namely, one of the direction cosines ($i = 1$) dominates the spectrum of cosines (i.e., $\lim_{N\to\infty} \cos^2\theta_{1,N} = 1$) and the rest of the cosines go to zero as N increases. In other words, in the large N limit, we have

$$W_L(N) = \cos^2\theta_{1,N} = 1 \text{ and } |L| = 1, \tag{S10.6}$$

in which $|L|$ is the number of elements (cardinality) of the set L.

On the other hand, if $I_0(N) = \mathbf{f}'_N(s)^{\mathrm{T}}(\mathbf{\Sigma}^0_N)^{-1}\mathbf{f}'_N(s)$ is unbounded only for specific stimuli or $\mathbf{f}'_N(s)$ is spanned in the subspace of $\mathbf{\Sigma}^0_N$, not all $\gamma_{i,N}$s are sublinear functions. If there exist multiple $\gamma_{i,N}$s that are linear functions of N and their respective eigenvectors are not orthogonal to $\mathbf{f}'_N(s)$, then $\mathbf{f}'_N(s)$ is spanned by these multiple eigenvectors of $\mathbf{\Sigma}_N$.

Supplementary Note 10: Subspace analysis by partial least squares may incorrectly report saturated LFI

In this section, we show that analyzing LFI using a dimension-reduction method, known as the Partial Least Squares (PLS) discriminant analysis, can result in an incorrect conclusion about its boundedness, while our method correctly predicts its behavior in the large N limit.

The PLS discriminant analysis identifies directions within a subspace of measurements that most effectively discriminate between two stimuli. The study by Rumyantsev et al.[1] applied the PLS analysis to distill the high-dimensional neural space into a latent space of five dimensions given by principal eigenvectors. They discovered that the eigenvector most aligned with the signal direction linearly scaled with the population size across five examined mice, and concluded that these and other increasing eigenvalues with the population size are responsible for the saturated behavior of the LFI, denoted as d' in their analysis. However, the reduced subspace may be constructed by leading eigenvectors of the original space, whose associated eigenvalues may scale linearly. Thus, the LFI calculated only from the reduced subspace attributes all cosine directions to the linear eigenvalues, which may necessarily result in bounded LFI.

To test this hypothesis, we simulated neural populations exhibiting unbounded LFI theoretically. For this goal, for each population of size N, we constructed N eigenvalues from the eigenspectrum given by Eq. 3 and 4 with the parameters derived from mouse TX42 whose estimated scaling parameter was $\alpha = 0.164 \pm 0.002$. To define angular occupations, we employed the relation between the angular occupation and eigenvalues given by Eq. 5 with an exponent $\gamma = 1$, which results in unbounded LFI for any $\alpha > 0$ (Supplementary Note 3).

More specifically, we constructed the covariance matrix $\mathbf{\Sigma}_N$ by associating random orthogonal vectors with the eigenvalues obtained from Eq. 3 and 4. To construct $\mathbf{f}_N(s)$ and $\mathbf{f}_N(s+\delta s)$, we assumed that the activity means are equal to the variance (i.e., the diagonal of $\mathbf{\Sigma}_N$). We then constructed $\mathbf{f}_N(s+\delta s) = \mathbf{f}_N(s) + \mathbf{f}'_N(s)\delta s$, where $\mathbf{f}'_N(s) = |\mathbf{f}'_N(s)| \sum_{i=1}^{N} \cos\theta_{i,N}\mathbf{u}_{i,N}$ is constructed using the $\cos^2\theta_{i,N}$ that comes from the power-law relation given by Eq. 5 using $\gamma = 1$. We then sampled neural activities from the Gaussian distribution $\mathcal{N}(\mathbf{f}_N(s), \mathbf{\Sigma}_N)$ and $\mathcal{N}(\mathbf{f}_N(s+\delta s), \mathbf{\Sigma}_N)$. The sample covariance matrix and signal for a subpopulation of size N were constructed from 2,600 samples (trials). The eigenspectra and angular occupations for subpopulation size N were obtained by averaging the results from 20 independently generated distributions.

The leading eigenvalues of the simulated dataset scale linearly as expected for $\alpha > 0$ (Extended Data Fig. 7a). As expected, the data shows the collapse of the eigenvalue spectrum by the scaling and shows the power-law relation between eigenvalues and angular occupations (Extended Data Fig. 7b,c). The scaling parameter and the slope were estimated as $\alpha = 0.203 \pm 0.0001$ and $\gamma = 1.009 \pm 0.011$. By applying the PLS method to the unbounded data, we find that the 10 eigenvalues extracted by the PLS method all scale linearly with population size (Extended Data Fig. 7d), and only partially recover the scaling behavior of the full system (Extended Data Fig. 7e,f).

Extended Data Figure 7g shows estimated LFI based on the PLS and our scaling-based method. The estimate of the LFI based on the PLS analysis (red) shows the saturated behavior, which follows the curve predicted by the differential correlations (dotted line). To the contrary, our scaling-based method (green) with estimated α and γ correctly predicts that the LFI of the population is unbounded (Extended Data Figure 7h). We note that the large eigenvalues from finite samples are biased upwards, compared to the original values[2]. While this results in the overestimation of α, using the estimated α is sufficient to conclude the unboundedness of the LFI because the critical γ_c is a decreasing function of α. For comparison, we provided the bias-corrected LFI estimate[3,4], which estimates the LFI precisely. However, we note that the method can not predict the behavior of LFI beyond the number set by the number of trials and neurons.

To further investigate the behavior of the PLS analysis, we simulated neural populations exhibiting unbounded LFI, assuming that the eigenvalues follow the scale-invariance given by Eq. 3 with $\alpha = 0$. We proved that the LFI of subsampled populations is unbounded under this condition

(Supplementary Note 4). All the eigenvalues, including the leading eigenvalues, scale sublinearly. We then sampled eigenvalues from the eigenspectrum given by Eq. 4 with the parameters derived from mouse TX42, except for α which we specified as $\alpha = 0$ and $\gamma = 1$, and $\mu = 0.5$. Note that we treated the parameter α in Eq. 4 as a separate parameter from the scaling parameter in Eq. 3, and this choice makes the limiting exponent of the power-law spectrum previously given by $1 + \alpha$ less than 1.

As expected, the leading eigenvalues of the sampled data scaled sublinearly (Extended Data Fig. 8a). The eigenvalue spectrum in the normalized indices shows the characteristic of $\alpha = 0$ for finite-size data. That is, the larger the population size, the larger the magnitude of the eigenvalues (Extended Data Fig. 8b) as discussed in Supplementary Note 4, from which we estimated α as zero. The fitted exponent γ was $\gamma = 0.968 \pm 0.016$ (Extended Data Fig. 8c), which is close to 1, but the error was larger than the previous example, possibly due to the lack of large magnitude of $\lambda_{i,N}$ because all eigenvalues scale sublinearly.

When we apply the PLS method to this data, we find that the largest eigenvalue scales closer to a linear line than the original eigenvalues (Extended Data Fig. 8d), despite the fact that there are no linearly scaling eigenvalues in the original data set. Similarly to the previous example, the method did not fully recover the scaling behavior present in the full systems. Accordingly, the estimate of the LFI based on the PLS analysis for this unbounded data shows again the saturated behavior (Extended Data Fig. 8g). While our scaling-based analysis correctly predicts that the LFI is unbounded (Extended Data Fig. 8h), it overestimated the LFI, which calls for a better parameter estimation method in the case of $\alpha = 0$.

References

[1] Rumyantsev, O. I. *et al.* Fundamental bounds on the fidelity of sensory cortical coding. *Nature* **580**, 100–105 (2020).

[2] Ledoit, O. & Wolf, M. A well-conditioned estimator for large-dimensional covariance matrices. *Journal of multivariate analysis* **88**, 365–411 (2004).

[3] Kanitscheider, I., Coen-Cagli, R., Kohn, A. & Pouget, A. Measuring fisher information accurately in correlated neural populations. *PLoS Comput. Biol.* **11**, e1004218 (2015).

[4] Kafashan, M. *et al.* Scaling of sensory information in large neural populations shows signatures of information-limiting correlations. *Nat. Commun.* **12**, 473 (2021).

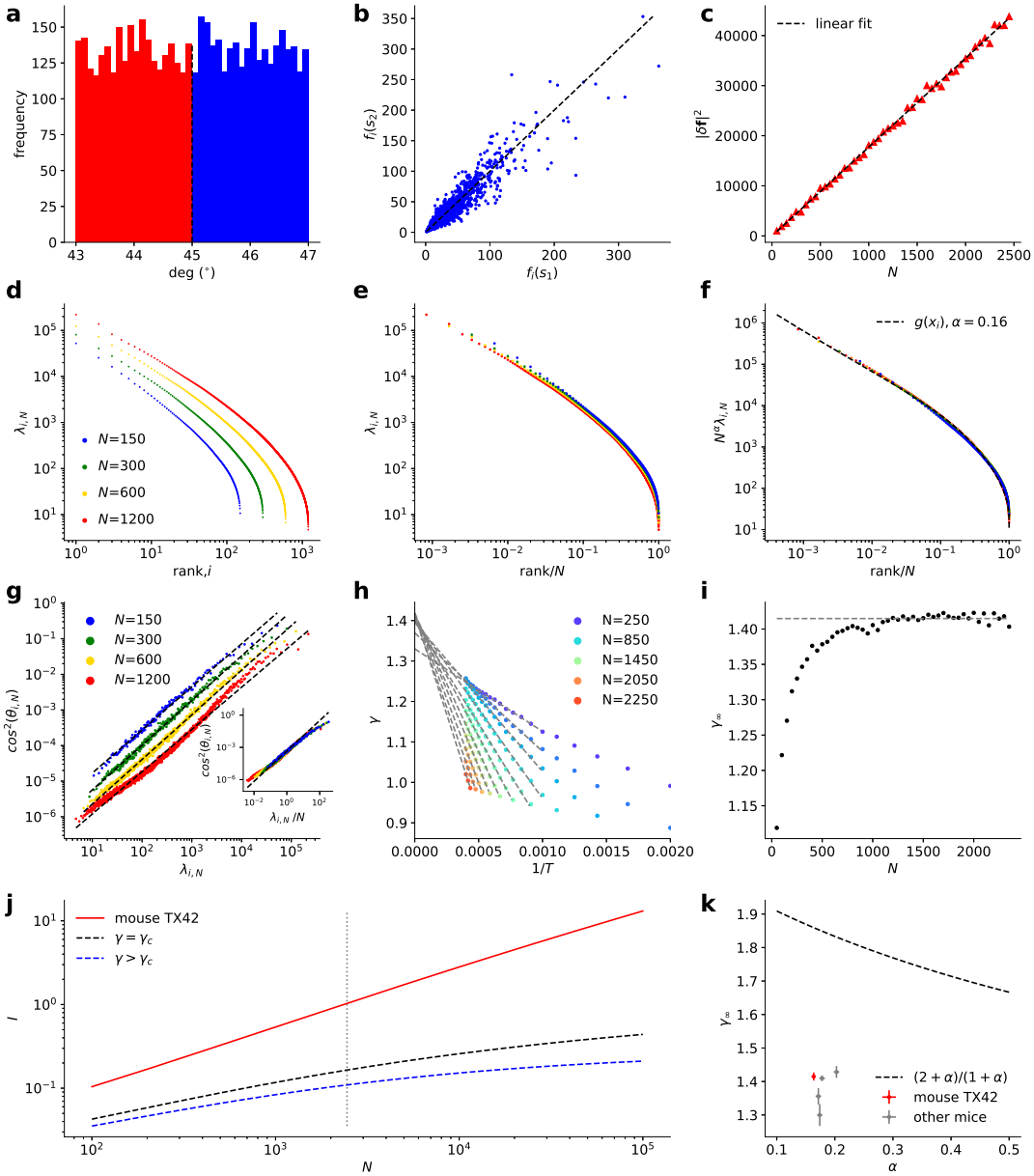

Extended Data Fig. 1. Analysis of mouse TX42. The figure styles follow Fig. 2 in the main text. The fitted scaling parameter is $\alpha = 0.164 \pm 0.002$. The fitted slope is $\gamma = 1.415 \pm 0.006$. **a**, A frequency histogram of gratings stimulus orientations. **b**, Comparison of mean responses of neurons $f_i(s)$ to the Stimulus 1 and 2. **c**, $|\delta f_i|^2$ vs the subpopulation size N. **d**, Noise eigenspectra for different N. **e**, The eigenspectra vs the normalized rank, $(x_i =)i/N$. **f**, The re-scaled eigenspectra by multiplying N^α. The dashed line is the fitted $g(x_i)$. **g**, $\cos^2\theta_{i,N}$ vs $\lambda_{i,N}$ for different N. The dashed lines are linear fit. (Inset) $\cos^2\theta_{i,N}$ vs the scaled eigenvalue, $\lambda_{i,N}/N$. **h**, The fitted γ as a function of $1/T$ for different N. The solid lines are fitted linear functions. **i**, The intercept γ_∞ for different N. The average γ_∞ (dashed line) was 1.415 ± 0.006. **j**, The inferred LFI (solid line) as a function of N in the log-log plot. The dashed lines are theoretical LFI. **k**, The estimated γ_∞ vs α. The dashed line is a critical boundary.

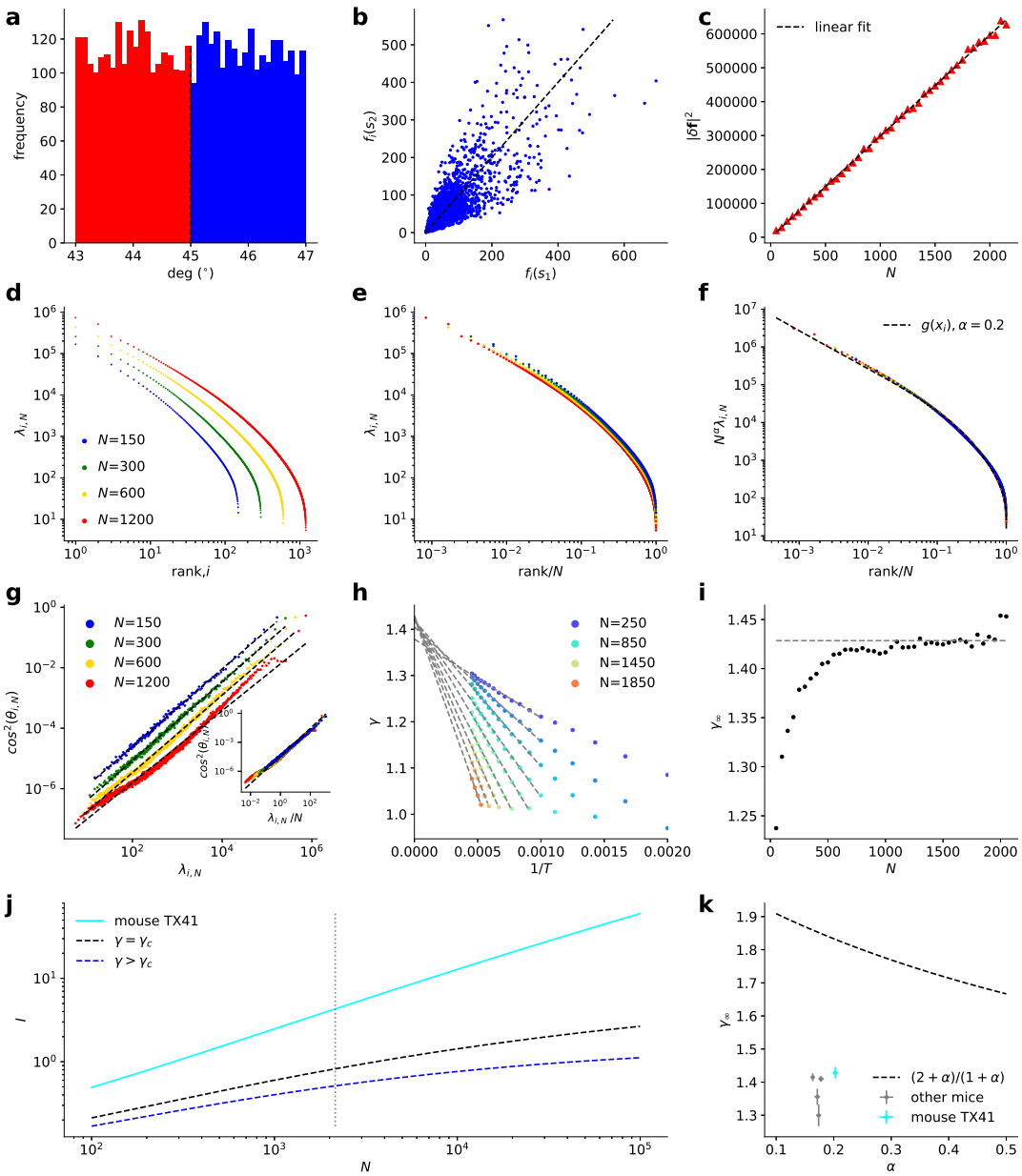

Extended Data Fig. 2. Analysis of mouse TX41. The figure style follows Fig. 5. The fitted scaling parameter is $\alpha = 0.203 \pm 0.002$. The fitted slope is $\gamma = 1.428 \pm 0.009$.

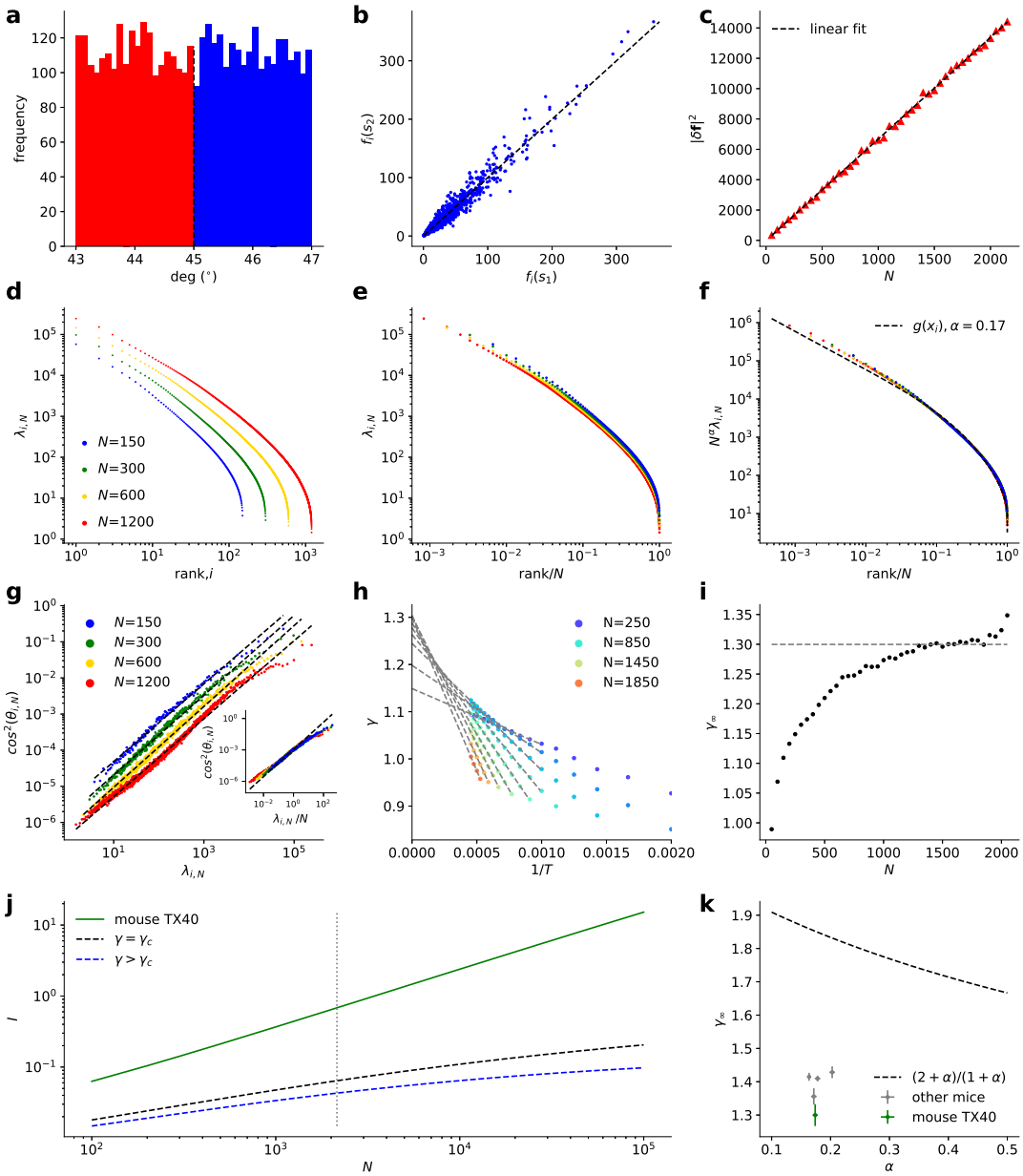

Extended Data Fig. 3. Analysis of mouse TX40. The figure style follows Fig. 5. The fitted scaling parameter is $\alpha = 0.174 \pm 0.002$. The fitted slope is $\gamma = 1.3 \pm 0.016$.

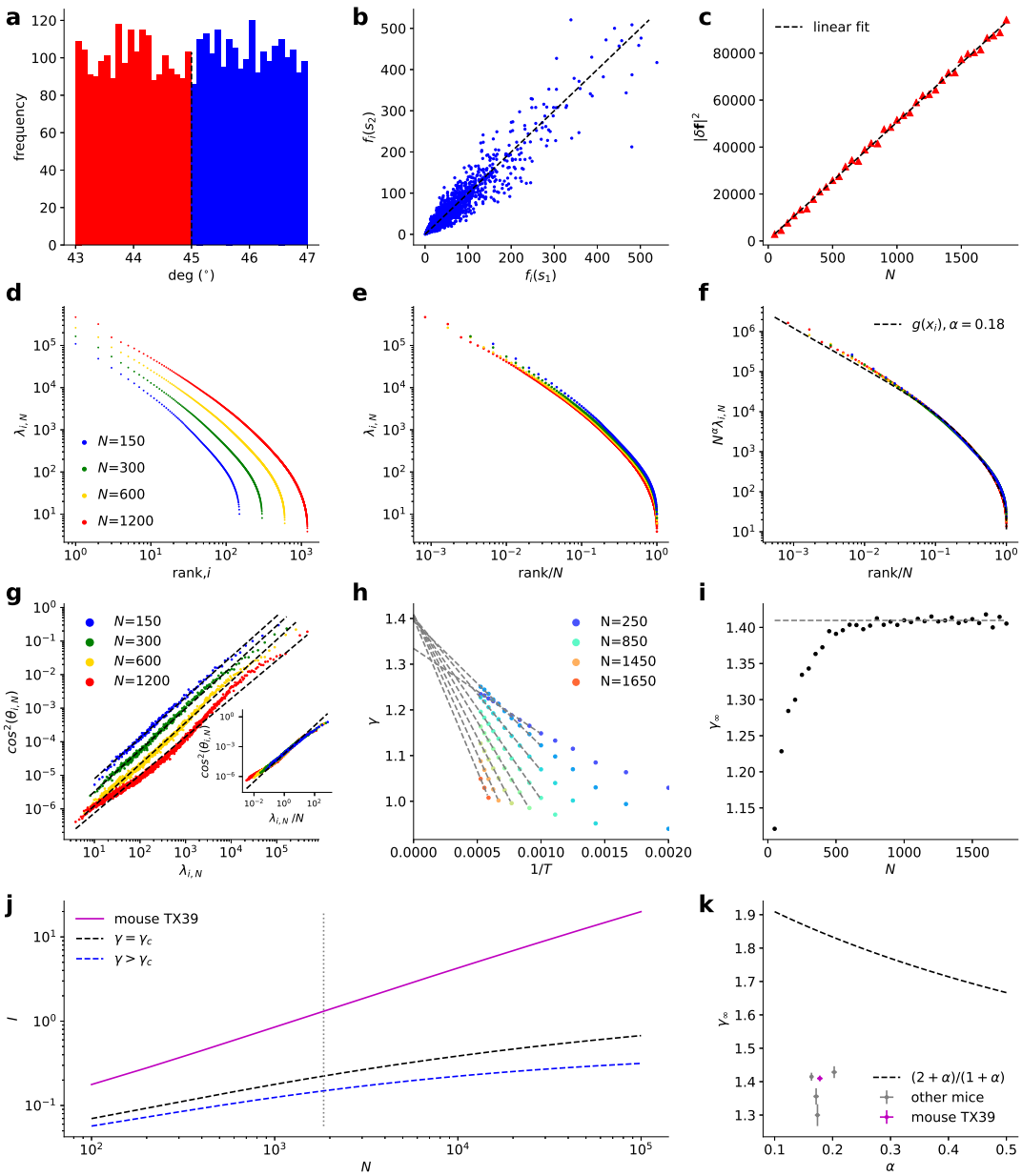

Extended Data Fig. 4. Analysis of mouse TX39. The figure style follows Fig. 5. The fitted scaling parameter is $\alpha = 0.178 \pm 0.002$. The fitted slope is $\gamma = 1.41 \pm 0.004$.

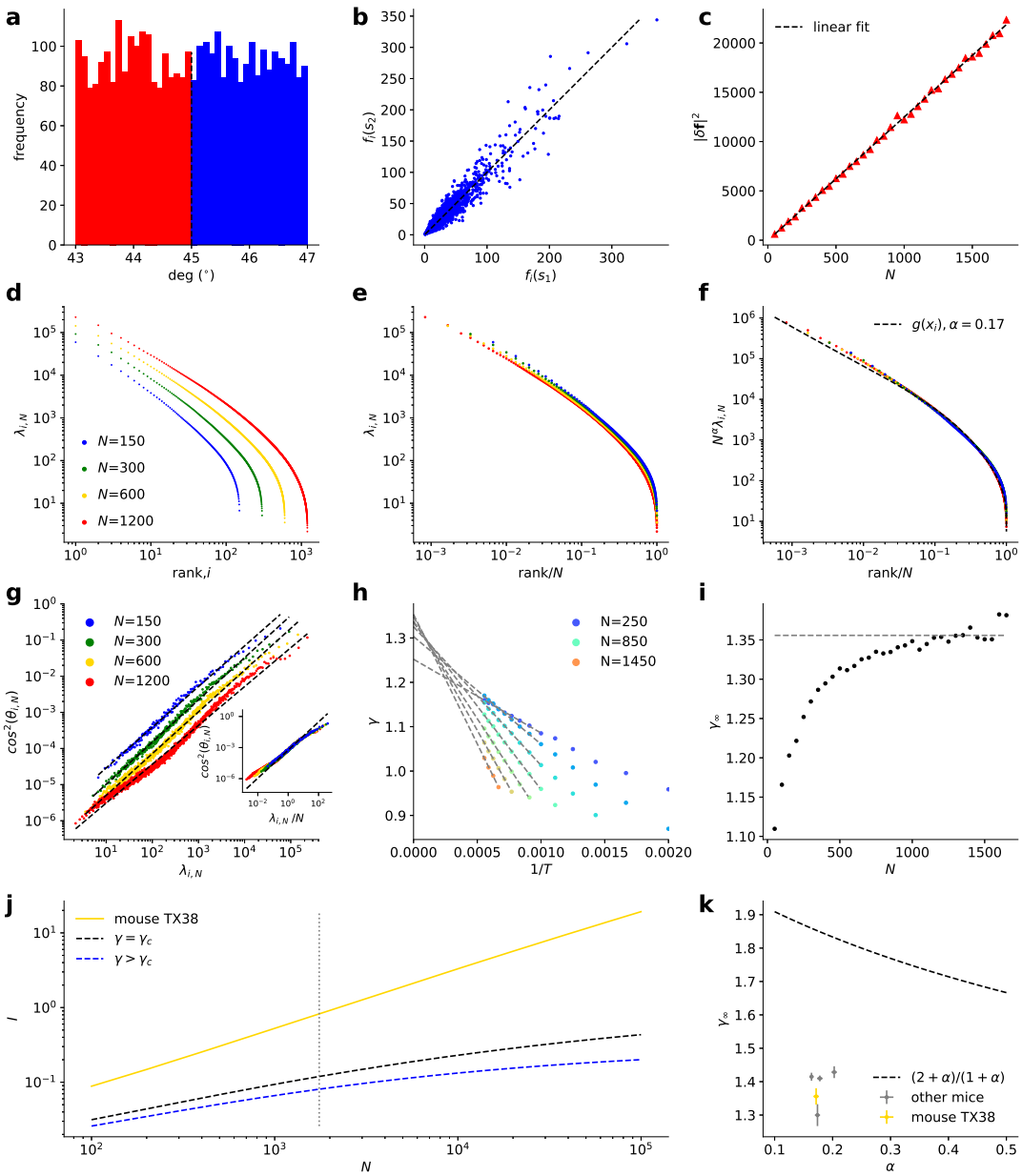

Extended Data Fig. 5. Analysis of mouse TX38. The figure style follows Fig. 5. The fitted scaling parameter is $\alpha = 0.172 \pm 0.002$. The fitted slope is $\gamma_\infty = 1.356 \pm 0.012$.

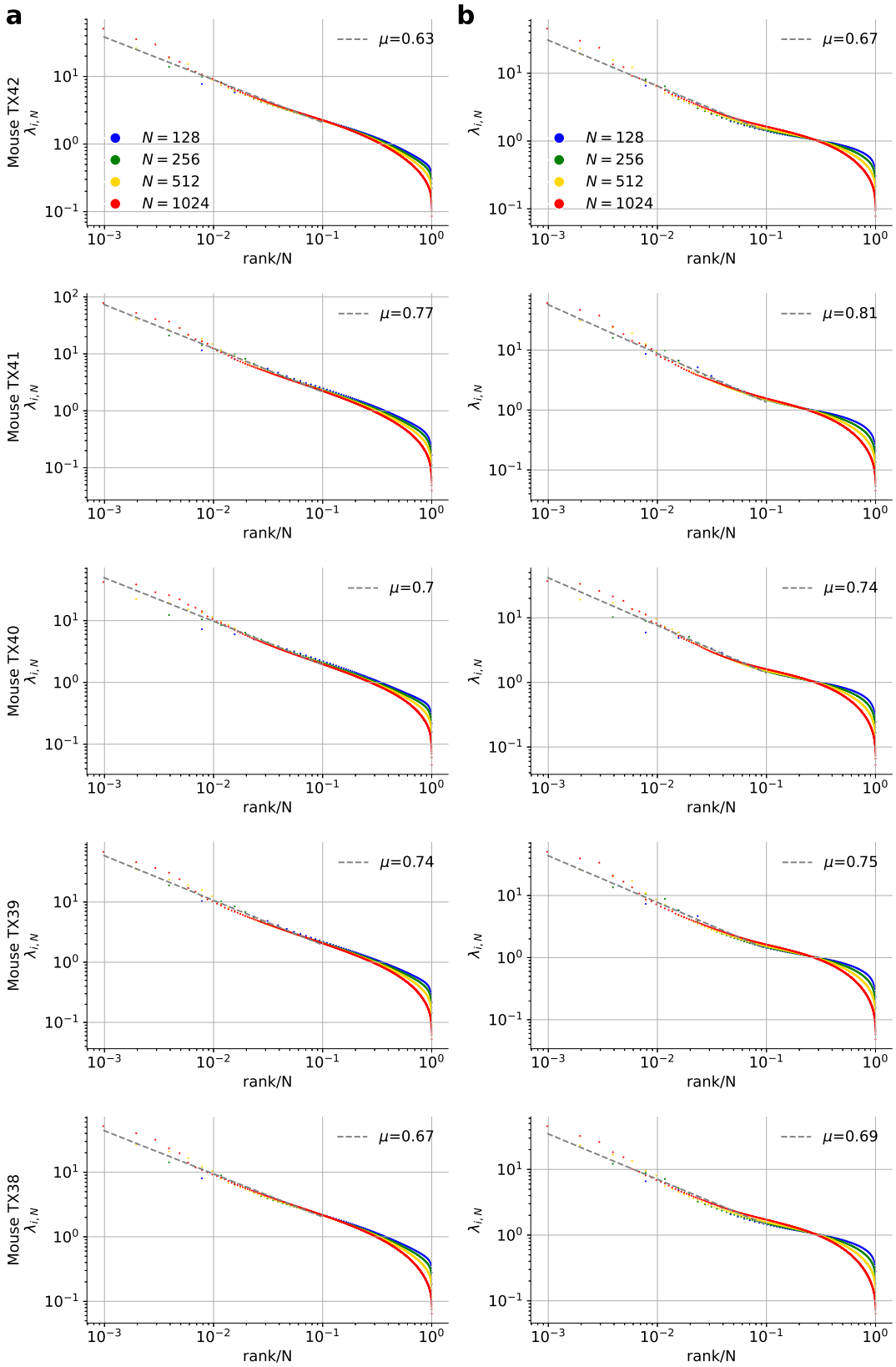

Extended Data Fig. 6. Eigenspectra of normalized covariance matrices for all mice. a Eigenspectra of covariances of the activity normalized by non-zero mean for each neuron (Slope: $\mu = 0.70 \pm 0.05$SD). The color stands for $N = 128, 256, 512, 1024$ **b** Eigenspectra of correlation coefficient matrices (Slope: $\mu = 0.73 \pm 0.05$SD)

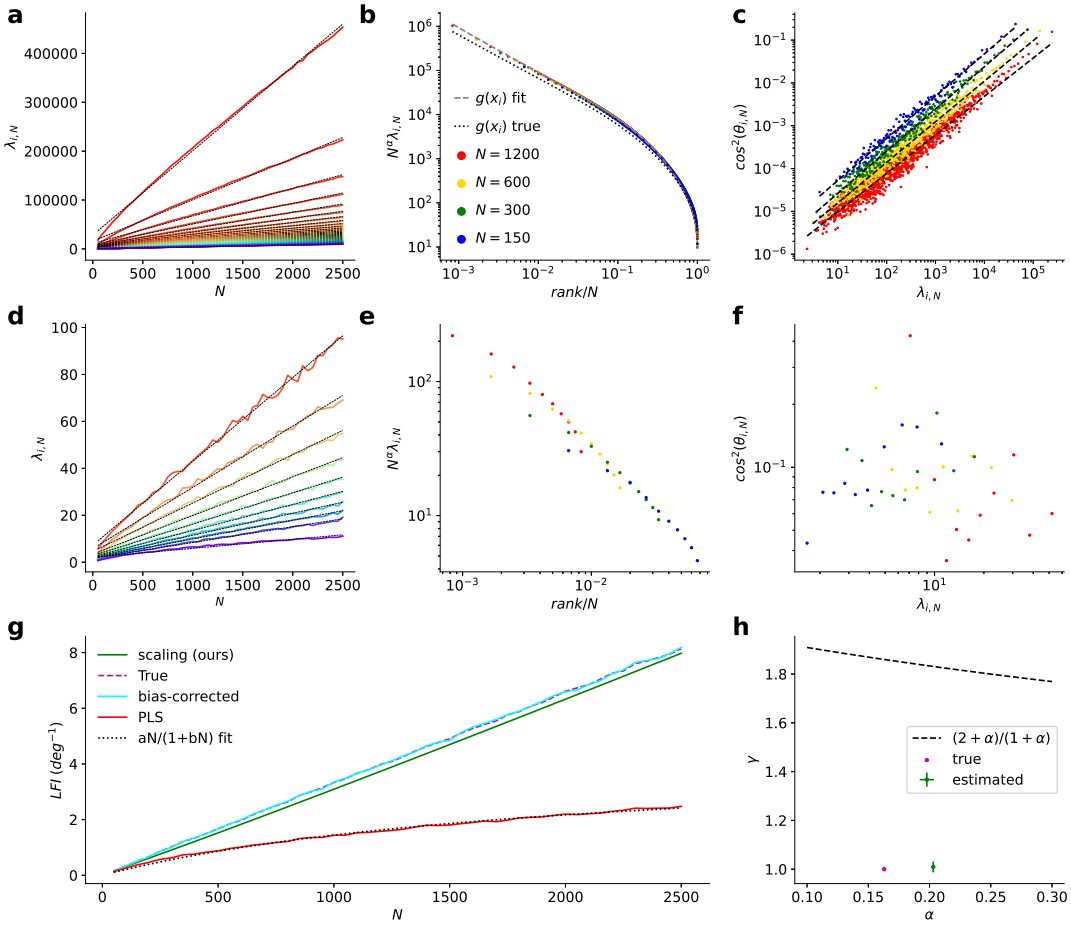

Extended Data Fig. 7. Comparison of the PLS analysis with the proposed scaling-based method using simulated data with non-zero α. The simulated data was generated from the eigenspectrum fitted to mouse TX42 ($\alpha = 0.163$). The angular occupation was obtained using Eq. 5 with $\gamma = 1$. **a**, The eigenvalues as a function of population size N. Only the largest 50 eigenvalues are shown. The leading eigenvalues scale linear for $\alpha > 0$. The black lines are linear fit. **b**, The collapsed eigenspectrum of the simulated data (colored dots) with the true (dotted) and fitted (dashed) eigenspectra. The fitted α is $\alpha = 0.203 \pm 0.0001$. **c**, The relation between the sampled eigenvalues and angular occupations. The estimated γ by the extrapolation method (see main text) is $\gamma = 1.009 \pm 0.011$. **d**, The eigenvalues of the 10-dimensional subspace obtained by the PLS method as a function of population size N. The black lines are linear fit. **e**, The collapsed eigenspectrum of the subspaces obtained by the PLS method. **f**, The relation between the sampled eigenvalues and angular occupations in the subspaces obtained by the PLS method. **g**, Comparison of the LFI estimated by the scaling-based method (green) and PLS method (red) with the true LFI (dashed magenta). The PLS method underestimates the LFI with a good fit by the bounded function $aN/(1+bN)$ (dotted black), while the scaling-based method correctly estimates the true unbounded LFI. For comparison, the bias-corrected estimate of LFI is shown (cyan). **h**, The estimated γ_∞ vs α by the scaling-based method. The dotted line is a critical boundary (Eq. 6), below which the LFI is unbounded. The error bars are 2SD.

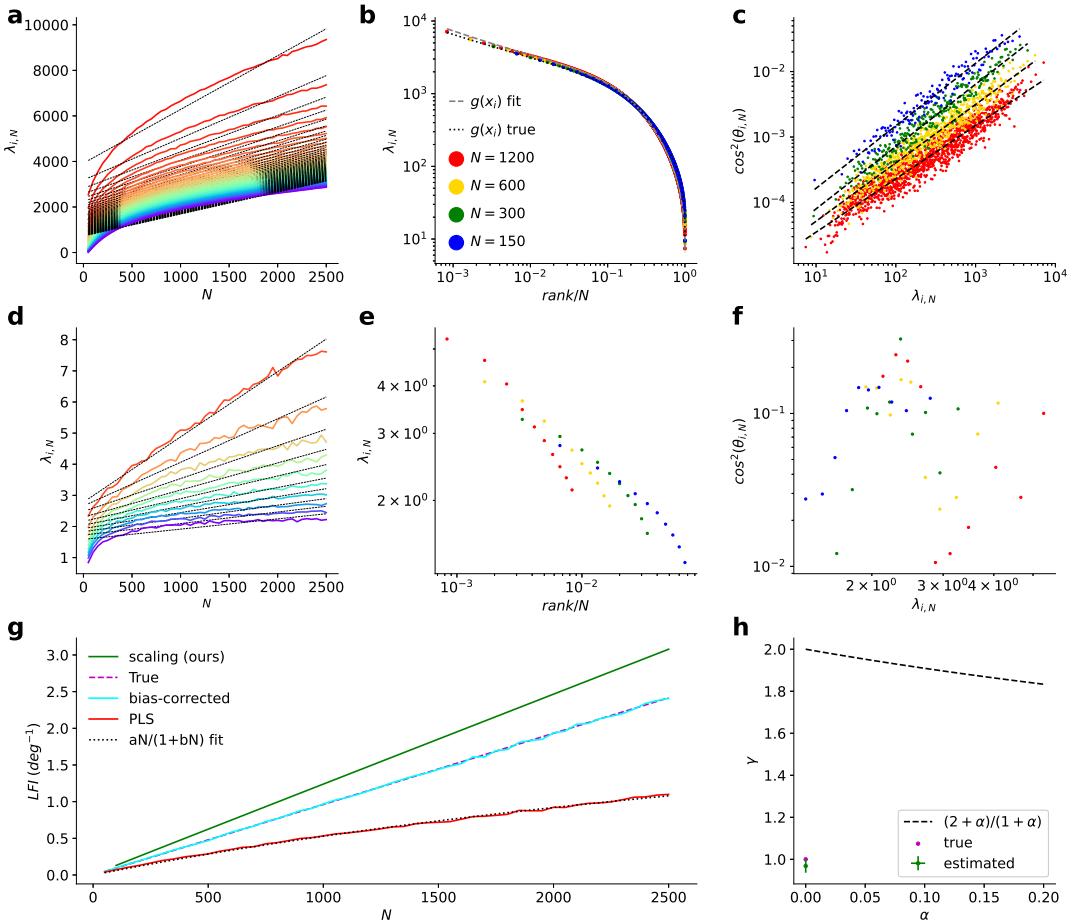

Extended Data Fig. 8. Comparison of the PLS analysis with the proposed scaling-based method using simulated data with $\alpha = 0$. The same analysis as in Fig. 7, but with simulated data using $\alpha = 0$. The simulated data was generated from the eigenvalue spectrum using $\alpha = 0$ and $g(x)$, in which we used parameters fitted to mouse TX42 except for the power-law exponent for which we used 0.5. The angular occupation was obtained using Eq. 5 with $\gamma = 1$. **a**, The eigenvalues as a function of population size N. Only the largest 50 eigenvalues are shown. All the eigenvalues scale sublinearly for $\alpha = 0$. The black lines are linear fit. **b**, The eigenspectrum of the simulated data (colored dots) with the true (dotted) and fitted (dashed) eigenspectra. Note that we observe the large eigenspectrum for a larger population size, indicating $\alpha = 0$. **c**, The relation between the sampled eigenvalues and angular occupations. The estimated γ by the extrapolation method (see main text) is $\gamma = 0.968 \pm 0.016 SD$. **d**, The eigenvalues of the 10-dimensional subspace obtained by the PLS method as a function of population size N. One of the subspace eigenvalues scales linearly. The black lines are linear fit. **e**, The collapsed eigenspectrum of the subspaces obtained by the PLS method. **f**, The relation between the sampled eigenvalues and angular occupations in the subspaces obtained by the PLS method. **g**, Comparison of the LFI estimated by the scaling-based method (green) and PLS method (red) with the true LFI (dashed magenta). The PLS method underestimates the LFI with a good fit by the bounded function $aN/(1+bN)$ (dotted black). The scaling-based method overestimates the true unbounded LFI. For comparison, the bias-corrected estimate of LFI is shown (cyan). **h**, The estimated γ_∞ vs α by the scaling-based method. The dotted line is a critical boundary (Eq. 6), below which the LFI is unbounded. The error bars are 2SD.